ELSEVIER

Journal of Quantitative Spectroscopy & Radiative Transfer 96 (2005) 205–239

Journal of Quantitative Spectroscopy & Radiative Transfer

www.elsevier.com/locate/jqsrt

Semi-empirical calculation of air-broadened half-widths and air pressure-induced frequency shifts of water-vapor absorption lines

David Jacquemart[a,1], Robert Gamache[b], Laurence S. Rothman[a,*]

[a]*Atomic and Molecular Physics Division, Harvard-Smithsonian Center for Astrophysics, Cambridge, MA 02138-1516, USA*

[b]*Department of Environmental, Earth & Atmospheric Sciences, University of Mass. Lowell, Lowell, MA 01854, USA*

Received 27 August 2004; received in revised form 30 November 2004; accepted 30 November 2004

Abstract

This paper describes a semi-empirical calculation of the air-broadened half-widths and the air pressure-induced frequency shifts for the $H_2^{16}O$ isotopologue. This semi-empirical calculation is based on fits of several recent high-quality measurements and theoretical calculations to the first-order terms in the expansion of the complex Robert–Bonamy (CRB) equations, which yields a second- and first-order polynomial function of the differences in the upper- and lower-state vibrational quantum numbers for the half-width and line shift, respectively. The aim of this work was to obtain a complete set of air-broadened half-widths and air pressure-induced frequency shifts for transitions of $H_2^{16}O$ present in the *HITRAN* database from microwave to the visible in order to supplement the observed and calculated values. For around 700 sets of rotational quantum numbers ($J'K'_aK'_c \leftarrow J''K''_aK''_c$), semi-empirical coefficients describing the vibrational dependence of the air-broadened half-widths and the air pressure-induced frequency shifts have been obtained directly from the fit of experimental and/or theoretical data. The accuracy of the parameters deduced from this calculation is estimated to be between 5% and 10% for the air-broadened half-widths and between 0.001 and 0.01 $cm^{-1}\,atm^{-1}$ for the air pressure-induced frequency shifts. For sets of rotational quantum numbers for which either none or insufficient experimental/

*Corresponding author. Tel.: +1 617 495 7474; fax: +1 617 496 7519.

E-mail address: lrothman@cfa.harvard.edu (L.S. Rothman).

[1]Laboratoire de Dynamique, Interactions et Réactivités, Université Pierre et Marie Curie, 4 Place Jussieu, Paris 75252, France.

0022-4073/$ - see front matter
doi:10.1016/j.jqsrt.2004.11.018

theoretical data were available to deduce a vibrational dependence, further approximations have been used to obtain a complete set of semi-empirical coefficients.

Keywords: Water-vapor absorption; Air-broadened half-width; Air pressure-induced line shift; Line shape

1. Introduction

Interpretation of atmospheric spectra requires high-precision line parameters describing line positions, intensities, pressure-broadened half-widths, and line shifts of gases present in the terrestrial atmosphere. Of these gases, water vapor is one of the most important greenhouse gases in the terrestrial atmosphere. Due to its relatively strong dipole moment, it is a major atmospheric absorber of infrared radiation with over 60,000 significant transitions ranging from the microwave region to the visible, of which about half are for the principal isotopologue $H_2^{16}O$. Accurate line parameters of water vapor are needed for remote sensing of this molecule, but also for their impact on other molecules since water-vapor transitions are often present in the channels used to detect and quantify other trace species.

Among the fundamental spectral parameters needed for terrestrial atmospheric radiative models (used to model natural radiative processes and to interpret remote-sensing data), there remain many deficiencies for the air-broadened half-widths, γ_{air}, and the air pressure-induced line shifts, δ_{air}. The goal of this work is to give a complete set of semi-empirical coefficients in order to calculate the γ_{air} and δ_{air} parameters of any rovibrational transition of the $H_2^{16}O$ isotopologue in order to update these parameters for the 2004 edition of the *HITRAN* database [1]. For the other isotopologues of water vapor, the number of references for the air-broadened half-widths and especially for the air pressure-induced frequency shifts is currently too small to determine the vibrational dependence of γ_{air} and δ_{air}.

Advances in the spectroscopy of water vapor and its key role in atmospheric and astrophysical studies have recently been reviewed [2]. The air-broadened half-widths for water vapor show a greater dynamic range and variability of values compared with other molecular absorbers in the atmosphere. The spectral line parameters used for remote-sensing simulations are usually obtained from the *HITRAN* database [1]. Because the preliminary positions, intensities, and assignment of the new *HITRAN* edition [1] were available, we used this version in order to set up a complete set of transitions for $H_2^{16}O$, for which we generated air-broadened half-widths and air pressure-induced frequency shifts. In the previous *HITRAN* [3], the γ_{air} parameters for the $H_2^{16}O$ isotopologue were selected from an assortment of about 300 measurements [4–7] and 2500 theoretical calculations [8] that are independent of the vibrational transition as well as a small number of vibrationally dependent measurements [6,7]. For other transitions, the γ_{air} parameters were estimated using scaled average values as a function of the rotational quantum number J [9]. Theoretical progress in the complex Robert–Bonamy theory (CRB) [10] to include the imaginary terms in the calculation of pressure-broadened half-widths [11] led to the prediction of vibrational dependence of the half-width, which is now confirmed by measurement [12]. Gamache and Hartmann [12] have demonstrated that the vibrational dependence can easily be modeled by a simple function. This dependence is shown in Fig. 1,

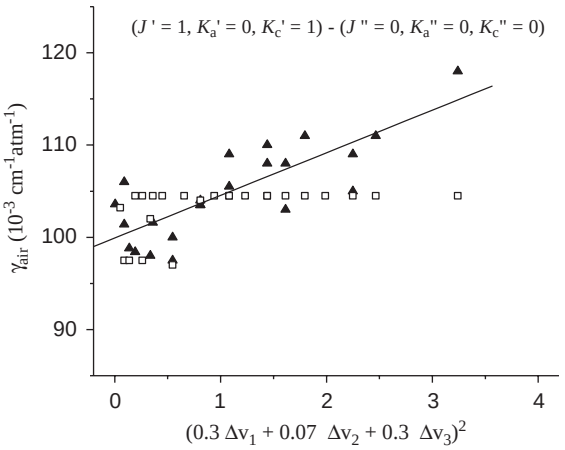

Fig. 1. Illustration of the vibrational dependence of experimental results of the air-broadening half-width for the $1_{01} \leftarrow 0_{00}$ transition (black triangles), symbolized by the linear fit of these experimental points (continuous line). The air-broadening half-widths from the previous *HITRAN* database [1] are represented by open squares. Note that the previous *HITRAN* database neglected the vibrational dependence of these coefficients.

where measured half-widths for the $1_{01} \leftarrow 0_{00}$ rotational transition are plotted versus the vibrational transition index described below. Also in the figure are the previous *HITRAN* [3] values (open squares). Note that most of the *HITRAN* [3] values were constant due to the neglect of vibrational dependence.

The values of γ_{air} for the main isotopologue $H_2^{16}O$ have been used for the $H_2^{18}O$ and $H_2^{17}O$ isotopologues assuming no isotopologue dependence for these parameters. This assumption has recently been validated with the theoretical work of Gamache and Fischer [13]. Parameters for the other isotopologues are discussed elsewhere [1].

New measurements [7,14–17] and theoretical calculations [12,13,18] both for γ_{air} and δ_{air} have recently been obtained, primarily for the main isotopologue $H_2^{16}O$. However, these data are not sufficient to obtain a complete set of γ_{air} and δ_{air} for many rovibrational transitions present in *HITRAN*. This is mainly due, first to the large number of transitions for water vapor, and second to the difficulty of having an accurate model for the rotational dependence of these parameters. Our study is based on a vibrational dependence model given by Gamache and Hartmann [12]. However, such a model applies only to a specific set of rotational quantum numbers (rotational quantum numbers of the lower and upper state of the transitions), which means that a vibrational study must be carried out for each set of rotational quantum numbers.

This paper is divided into 5 sections. Section 2 describes the equations used to model the vibrational dependence of γ_{air} and δ_{air}. Section 3 summarizes the set of measurements and theoretical calculations used for the fits leading to the semi-empirical coefficients describing the vibrational dependence of these parameters. Section 4 describes the methodology used to obtain a complete set of semi-empirical coefficients needed to calculate γ_{air} and δ_{air} for any rovibrational transition. Finally, Section 5 presents comparisons between our calculated values with measurement and theory.

2. Model of vibrational dependence for the air-broadened half-widths and the air pressure-induced frequency shifts

The theoretical concept used in this work for the vibrational dependence of $\gamma_{\rm air}$ and $\delta_{\rm air}$ was taken from the work of Gamache et al. [11,12,19] based on the CRB formalism [10]. Considering an isolated rovibrational transition $(v_1', v_2', v_3')f \leftarrow (v_1'', v_2'', v_3'')i$, where the v_k represent the quantum numbers associated with the normal mode of vibration k and the primes and double primes are, respectively, used for the upper and lower level, and i and f are the rotational quantum numbers of the transition. The line shift δ, and half-width γ, are given respectively, by the negative of the imaginary part and by the real part of the diagonal element of the complex relaxation matrix. Expanding the sine and cosine terms in the CRB equations, keeping only the first-order terms, and realizing that the vibrational dependence of the polarizability dominates the vibrational dephasing term, yields approximate expressions for γ and δ for a transition involving various vibrational states but specific sets i and f of rotational quantum numbers. These expressions have the following dependence on vibration quantum numbers [12]:

$$\gamma[(v_1', v_2', v_3')f \leftarrow (v_1'', v_2'', v_3'')i] = \gamma^0_{f\leftarrow i} + A_{f\leftarrow i} \times (0.3\Delta v_1 + 0.07\Delta v_2 + 0.3\Delta v_3)^2, \quad (1)$$

$$\delta[(v_1', v_2', v_3')f \leftarrow (v_1'', v_2'', v_3'')i] = \delta^0_{f\leftarrow i} + B_{f\leftarrow i} \times (0.3\Delta v_1 + 0.07\Delta v_2 + 0.3\Delta v_3), \quad (2)$$

where Δv_i is equal to $v_i' - v_i''$. For water vapor, the notation i and f corresponds, respectively, to the rotational quantum numbers $(J'', K_{\rm a}'', K_{\rm c}'')$ and $(J', K_{\rm a}', K_{\rm c}')$. $\gamma^0_{f\leftarrow i}$ and $\delta^0_{f\leftarrow i}$ are equivalent respectively to the half-width and line shift for a pure rotational transition which corresponds to the transition $(v_1' = 0, v_2' = 0, v_3' = 0)f \leftarrow (v_1'' = 0, v_2'' = 0, v_3'' = 0)i$. In the following we will denote the semi-empirical coefficients as $\gamma^0_{f\leftarrow i}$, $A_{f\leftarrow i}$, $\delta^0_{f\leftarrow i}$, and $B_{f\leftarrow i}$, where $\gamma^0_{f\leftarrow i}$ and $\delta^0_{f\leftarrow i}$ are the intercepts, and $A_{f\leftarrow i}$ and $B_{f\leftarrow i}$ are the slopes of the fits of Eqs. (1) and (2) to determine the vibrational dependence.

The vibrational dependence of $\gamma_{\rm air}$ and $\delta_{\rm air}$ for water vapor is modeled using Eqs. (1) and (2). These two equations indicate a quadratic and linear dependence on the quantity $\Delta v = (0.3\Delta v_1 + 0.07\Delta v_2 + 0.3\Delta v_3)$ for $\gamma_{\rm air}$ and $\delta_{\rm air}$, respectively. The semi-empirical coefficients are determined as a function of the rotational quantum numbers of a transition. Once the coefficients are determined, $\gamma_{\rm air}$ and $\delta_{\rm air}$ may be calculated for any rovibrational transition with the same set of rotational quantum numbers. The two intercepts $\gamma^0_{f\leftarrow i}$ and $\delta^0_{f\leftarrow i}$ are determined mainly from the air-broadened half-widths and the air pressure-induced frequency shifts in the microwave region and in the far and mid-infrared ($<3000\,{\rm cm}^{-1}$). The two slopes $A_{f\leftarrow i}$ and $B_{f\leftarrow i}$ are determined mainly from $\gamma_{\rm air}$ and $\delta_{\rm air}$ in the near infrared or the visible. In order to have accurate values of these semi-empirical coefficients, a large variety of experimental and/or theoretical data are needed to make the fits.

3. Observed and theoretically calculated data used to determine semi-empirical coefficients

For the analysis of the vibrational dependence of the $\gamma_{\rm air}$ and $\delta_{\rm air}$ parameters of water vapor, we decided to select from the literature a limited set of recent high-quality measurements and

theoretical calculations covering the whole water-vapor spectrum from microwave through visible. The first criterion was to choose studies for which a large number of results on both γ_{air} and δ_{air} have been obtained. However, for the air pressure-induced frequency shifts of $H_2^{16}O$, one observes a crucial lack of references between 2000 and 8000 cm^{-1} since only three works have been published [14,17,20] (Note that Ref. [20] deals only with N_2-broadening and shift parameters).

Finally, among all the works available in the literature, we selected three theoretical studies, and five experimental works. The three theoretical calculations have been made by Gamache et al. [12,13,18] using the CRB formalism, and the experimental data come from different studies [7,14–17] using high-resolution spectra recorded with Fourier transform spectrometers.

For the microwave spectral region and the far infrared below 500 cm^{-1}, we used the calculations of air-broadened half-widths for pure rotational transitions from Gamache and Fischer [13]. For the infrared spectral region, several works on both γ_{air} and δ_{air} have been used: the calculations from Gamache and Hartmann [12] between 500 and 4200 cm^{-1}, the measurements from Zou and Varanasi [17] between 1270 and 4200 cm^{-1}, and the measurements from Toth [14] between 600 and 7800 cm^{-1}. Note that the recent work of Toth [14] summarizes the extensive studies done by the author on water vapor, but also presents new measurements, especially for air-broadening and shift parameters for transitions above 2800 cm^{-1}.

For the near-infrared and visible spectral regions, four studies of both γ_{air} and δ_{air} have been used: the measurements of Mérienne et al. [16] between 9250 and 12,750 cm^{-1}, of Brown et al. [7] between 10,150 and 11,190 cm^{-1}, the calculations of Gamache and Fischer [18] between 13,300 and 14,300 cm^{-1}, and the experimental results of Fally et al. [15] between 13,370 and 22,640 cm^{-1}.

A detailed summary of the measurements and the theoretical calculations used in this work for the study of the vibrational dependence of γ_{air} and δ_{air} for $H_2^{16}O$ is presented in Table 1. The number of measurements or calculations for each vibrational band is presented. The total number of experimental and theoretical data used in this work for both γ_{air} and δ_{air} is around 15,000. A sample of these data, sorted by rotational quantum numbers, is given in Table 2. This sample represents all the experimental and theoretical data from Refs. [7,12–18] for just four sets of rotational quantum numbers: $1_{01} \leftarrow 0_{00}$, $1_{11} \leftarrow 0_{00}$, $0_{00} \leftarrow 1_{01}$, and $1_{10} \leftarrow 1_{01}$.

4. Determination of a complete set of semi-empirical coefficients

This section describes how a complete set of semi-empirical coefficients describing the vibrational dependence of air-broadened half-widths and air pressure-induced frequency shifts of $H_2^{16}O$ was obtained. The complete set of semi-empirical coefficients allows one to calculate γ_{air} and δ_{air} for any rovibrational transition. This section is divided into two parts: in Section 4.1 we present the semi-empirical coefficients obtained directly from the fit of experimental and theoretical data using Eqs. (1) and (2), respectively, for γ_{air} and δ_{air}. Because the set of experimental and theoretical data was insufficient for modeling the vibrational dependence of all sets of rotational quantum numbers, it has been necessary to perform some additional approximations. These approximations are presented in Section 4.2.

Table 1
Summary of experimental and theoretical data used for modeling the vibrational dependence of the air-broadened half-widths and the air pressure-induced frequency shifts of $H_2^{16}O$

Spectral region (cm^{-1})	Type of data	Source	Total number of lines	$v'_1, v'_2, v'_3 - v''_1, v''_2, v''_3$ (number of lines for each vibrational band)
0–500	Calculation	[13]	453	000–000 (453)
500–4200	Calculation	[12]	3121	000–000 (535), 010–000 (2410), 100–000 (75), 001–000 (101)
1270–4020	Experimental	[17]	699	010–000 (324), 020–000 (18) 001–000 (239), 100–000 (118)
600–7800	Experimental	[14]	4160	000–000 (149), 010–010 (1), 010–000 (792), 020–010 (113), 100–010 (13),001–010 (27), 011–010 (9), 100–000 (368), 001–000 (494), 020–000 (367), 030–010 (5), 030–000 (61), 021–010 (25), 110–000 (171), 011–000 (458), 031–010 (2), 021–000 (248), 101–000 (350), 002–000 (128), 040–000 (5), 200–000 (226), 120–000 (144), 111–010 (4)
9250–12,750	Experimental	[16]	2347	111–000 (33), 012–000 (38), 210–000 (3), 041–000 (167), 220–000 (137), 131–010 (8), 121–000 (312), 022–000 (83), 300–000 (263), 003–000 (291), 201–000 (360), 102–000 (230), 211–010 (6), 310–010 (3), 131–000 (75), 112–000 (67), 211–000 (133), 310–000 (37), 013–000 (101)
10,150–11,190	Experimental	[7]	503	121–000 (108), 220–000 (1), 022–000 (2), 003–000 (86), 300–000 (77), 102–000 (38), 201–000 (191)
13,300–14,300	Calculation	[18]	561	221–000 (223), 301–000 (338)
13,370–22,640	Experimental	[15]	3877	061–000 (2), 160–000 (2), 042–000 (9), 240–000 (7), 141–000 (21), 122–000 (62), 023–000 (70), 221–000 (216), 320–000 (66), 400–000 (196), 301–000 (302), 202–000 (203), 103–000 (250), 004–000 (68), 071–000 (5), 170–000 (3), 151–000 (1), 132–000 (5), 033–000 (62), 231–000 (127), 330–000 (15),311–000 (236), 410–000 (134), 212–000 (59), 113–000 (143), 142–000 (52), 043–000 (8), 340–000 (17), 241–000 (17), 222–000 (23), 123–000 (59), 321–000 (135), 420–000 (76), 500–000 (144), 401–000 (407), 302–000 (113), 203–000 (142), 104–000 (16), 053–000 (8), 034–000 (3), 133–000 (8), 331–000 (78), 430–000 (5), 312–000 (1), 213–000 (47), 510–000 (49), 411–000 (91), 063–000 (4), 341–000 (31), 223–000 (3), 322–000 (9), 421–000 (10), 600–000 (60), 501–000 (118), 402–000 (3), 303–000 (24), 115–000 (1), 431–000 (3), 511–000 (21), 601–000 (19), 700–000 (8)

Note: The number of lines given in this table corresponds to the number of lines for which measurements or calculations have been determined approximately for both the air-broadened half-widths and the air pressure-induced frequency shifts.

Table 2
Sample of experimental and theoretical data used for modeling the vibrational dependence of the air broadening (γ_{air}) and the air-pressure shift (δ_{air}) coefficients

J'	K'_a	K'_c	J''	K''_a	K''_c	v'_1	v'_2	v'_3	v''_1	v''_2	v''_3	Δv	γ_{air}	δ_{air}	Ref.	%	Dif
1	0	1	0	0	0	0	1	0	0	0	0	0.07	103.58	−0.73	[12]	3.66	−1.96
1	0	1	0	0	0	0	0	1	0	0	0	0.30	101.40	−4.50	[17]	1.08	−1.54
1	0	1	0	0	0	0	0	1	0	0	0	0.30	106.00	−5.25	[14]	5.67	−2.29
1	0	1	0	0	0	0	1	1	0	0	0	0.37	98.80	−5.75	[14]	−1.72	−1.52
1	0	1	0	0	0	0	2	1	0	0	0	0.44	98.40	−3.58	[14]	−2.37	1.93
1	0	1	0	0	0	0	4	1	0	0	0	0.58	98.00	−6.00	[16]	−3.40	2.06
1	0	1	0	0	0	1	0	1	0	0	0	0.60	101.60	−5.66	[14]	0.04	2.76
1	0	1	0	0	0	1	2	1	0	0	0	0.74	97.50	−12.10	[7]	−4.80	−1.13
1	0	1	0	0	0	1	2	1	0	0	0	0.74	100.00	−16.00	[16]	−2.36	−5.03
1	0	1	0	0	0	1	3	1	0	0	0	0.81	62.00	−12.00	[16]	−39.76	0.24
1	0	1	0	0	0	2	0	1	0	0	0	0.90	103.50	−12.00	[7]	−0.12	1.88
1	0	1	0	0	0	0	0	3	0	0	0	0.90	104.00	−13.00	[16]	0.36	0.88
1	0	1	0	0	0	0	0	3	0	0	0	0.90	103.50	−14.20	[7]	−0.12	−0.32
1	0	1	0	0	0	0	1	3	0	0	0	0.97	102.00	−4.00	[16]	−2.14	11.15
1	0	1	0	0	0	2	2	1	0	0	0	1.04	109.00	−13.00	[15]	3.93	3.43
1	0	1	0	0	0	2	2	1	0	0	0	1.04	105.50	−8.77	[18]	0.60	7.66
1	0	1	0	0	0	0	2	3	0	0	0	1.04	87.00	−32.00	[15]	−17.04	−15.57
1	0	1	0	0	0	2	3	1	0	0	0	1.11	41.00	15.00	[15]	−61.16	32.70
1	0	1	0	0	0	3	0	1	0	0	0	1.20	108.00	−9.86	[18]	1.39	9.48
1	0	1	0	0	0	3	0	1	0	0	0	1.20	106.00	−20.00	[15]	−0.49	−0.66
1	0	1	0	0	0	1	0	3	0	0	0	1.20	110.00	−21.00	[15]	3.26	−1.66
1	0	1	0	0	0	3	1	1	0	0	0	1.27	108.00	−22.00	[15]	0.63	−1.39
1	0	1	0	0	0	1	1	3	0	0	0	1.27	103.00	−21.00	[15]	−4.02	−0.39
1	0	1	0	0	0	3	2	1	0	0	0	1.34	111.00	−22.00	[15]	2.63	−0.11
1	0	1	0	0	0	3	3	1	0	0	0	1.41	88.00	8.00	[15]	−19.30	31.16
1	0	1	0	0	0	4	0	1	0	0	0	1.50	105.00	−22.00	[15]	−4.76	2.80
1	0	1	0	0	0	2	0	3	0	0	0	1.50	109.00	−27.00	[15]	−1.13	−2.20
1	0	1	0	0	0	4	1	1	0	0	0	1.57	111.00	−23.00	[15]	−0.21	3.07
1	0	1	0	0	0	3	0	3	0	0	0	1.80	118.00	−37.00	[15]	2.78	−6.74
1	1	1	0	0	0	0	0	0	0	0	0	0.00	103.15		[13]	2.03	
1	1	1	0	0	0	0	1	0	0	0	0	0.07	102.00	3.25	[14]	0.89	−0.14
1	1	1	0	0	0	0	1	0	0	0	0	0.07	100.50	3.60	[17]	−0.60	0.21
1	1	1	0	0	0	0	1	0	0	0	0	0.07	101.50	3.15	[12]	0.39	−0.24
1	1	1	0	0	0	0	2	0	0	0	0	0.14	101.50	1.85	[14]	0.38	−0.53
1	1	1	0	0	0	1	0	0	0	0	0	0.30	102.90	−1.30	[17]	1.69	−1.38
1	1	1	0	0	0	1	0	0	0	0	0	0.30	98.00	0.25	[14]	−3.15	0.17
1	1	1	0	0	0	1	1	0	0	0	0	0.37	99.30	−1.61	[14]	−1.91	−0.68
1	1	1	0	0	0	2	0	0	0	0	0	0.60	102.20	−1.99	[14]	0.73	2.25
1	1	1	0	0	0	1	0	2	0	0	0	0.90	91.00	−7.00	[16]	−10.71	1.56
1	1	1	0	0	0	3	0	0	0	0	0	0.90	99.00	−7.20	[7]	−2.86	1.36
1	1	1	0	0	0	3	0	0	0	0	0	0.90	96.00	−8.00	[16]	−5.80	0.56
1	1	1	0	0	0	3	1	0	0	0	0	0.97	105.00	−7.00	[16]	2.90	2.57
1	1	1	0	0	0	3	2	0	0	0	0	1.04	101.00	1.00	[15]	−1.16	11.58
1	1	1	0	0	0	1	4	2	0	0	0	1.18	19.00	−13.00	[15]	−81.46	−0.41
1	1	1	0	0	0	0	0	4	0	0	0	1.20	49.00	−27.00	[15]	−52.21	−14.12
1	1	1	0	0	0	2	0	2	0	0	0	1.20	105.00	−3.00	[15]	2.40	9.88

Table 2 (*continued*)

J'	K'_a	K'_c	J''	K''_a	K''_c	v'_1	v'_2	v'_3	v''_1	v''_2	v''_3	Δv	γ_{air}	δ_{air}	Ref.	%	Dif
1	1	1	0	0	0	4	0	0	0	0	0	1.20	72.00	−22.00	[15]	−29.78	−9.12
1	1	1	0	0	0	4	1	0	0	0	0	1.27	101.00	−17.00	[15]	−1.67	−3.11
1	1	1	0	0	0	3	0	2	0	0	0	1.50	100.00	−40.00	[15]	−3.24	−22.80
0	0	0	1	0	1	0	1	0	0	0	0	0.07	104.41	−0.47	[12]	5.12	−3.02
0	0	0	1	0	1	0	0	1	0	1	0	0.23	98.30	−1.76	[14]	−1.25	−1.69
0	0	0	1	0	1	0	0	1	0	0	0	0.30	100.80	−2.00	[17]	1.08	−0.78
0	0	0	1	0	1	0	1	1	0	0	0	0.37	101.50	−2.98	[14]	1.56	−0.61
0	0	0	1	0	1	0	2	1	0	1	0	0.37	97.50	−1.80	[14]	−2.44	0.57
0	0	0	1	0	1	0	2	1	0	0	0	0.44	96.00	−1.25	[14]	−4.20	2.27
0	0	0	1	0	1	0	4	1	0	0	0	0.58	91.00	−10.00	[16]	−9.79	−4.19
0	0	0	1	0	1	1	0	1	0	0	0	0.60	102.60	−6.60	[14]	1.59	−0.46
0	0	0	1	0	1	1	2	1	0	0	0	0.74	99.40	−8.10	[7]	−2.43	0.34
0	0	0	1	0	1	1	2	1	0	0	0	0.74	105.00	−10.00	[16]	3.07	−1.56
0	0	0	1	0	1	0	7	1	0	0	0	0.79	98.00	−3.00	[15]	−4.14	6.26
0	0	0	1	0	1	1	3	1	0	0	0	0.81	99.00		[16]	−3.30	
0	0	0	1	0	1	2	0	1	0	0	0	0.90	62.00		[16]	−39.87	
0	0	0	1	0	1	0	0	3	0	0	0	0.90	103.50	−11.10	[7]	0.38	−0.04
0	0	0	1	0	1	2	0	1	0	0	0	0.90	93.90		[7]	−8.93	
0	0	0	1	0	1	0	0	3	0	0	0	0.90	83.00	−18.00	[16]	−19.50	−6.94
0	0	0	1	0	1	0	1	3	0	0	0	0.97	99.00	−7.00	[16]	−4.55	5.21
0	0	0	1	0	1	0	2	3	0	0	0	1.04	109.00	−13.00	[15]	4.42	0.36
0	0	0	1	0	1	2	2	1	0	0	0	1.04	112.00	19.00	[15]	7.30	32.36
0	0	0	1	0	1	2	2	1	0	0	0	1.04	107.20	−8.39	[18]	2.70	4.97
0	0	0	1	0	1	2	3	1	0	0	0	1.11	85.00	−7.00	[15]	−19.12	7.50
0	0	0	1	0	1	3	0	1	0	0	0	1.20	108.00	−13.00	[15]	1.82	2.98
0	0	0	1	0	1	3	0	1	0	0	0	1.20	108.70	−11.37	[18]	2.48	4.61
0	0	0	1	0	1	1	0	3	0	0	0	1.20	108.00	−19.00	[15]	1.82	−3.02
0	0	0	1	0	1	1	1	3	0	0	0	1.27	132.00	−2.00	[15]	23.50	15.13
0	0	0	1	0	1	3	1	1	0	0	0	1.27	109.00	−20.00	[15]	1.98	−2.87
0	0	0	1	0	1	1	2	3	0	0	0	1.34	81.00	−28.00	[15]	−24.82	−9.72
0	0	0	1	0	1	3	2	1	0	0	0	1.34	109.00	−21.00	[15]	1.17	−2.72
0	0	0	1	0	1	3	3	1	0	0	0	1.41	80.00	−20.00	[15]	−26.37	−0.58
0	0	0	1	0	1	2	0	3	0	0	0	1.50	111.00	−23.00	[15]	1.02	−2.10
0	0	0	1	0	1	2	1	3	0	0	0	1.57	93.00	−1.00	[15]	−16.13	21.05
0	0	0	1	0	1	4	1	1	0	0	0	1.57	128.00	−20.00	[15]	15.43	2.05
0	0	0	1	0	1	3	0	3	0	0	0	1.80	110.00	−28.00	[15]	−3.95	−2.18
0	0	0	1	0	1	6	0	1	0	0	0	2.10	197.00	−51.00	[15]	64.13	−20.26
1	1	0	1	0	1	0	0	0	0	0	0	0.00	109.28		[13]	5.58	
1	1	0	1	0	1	0	1	0	0	0	0	0.07	106.41	6.40	[12]	2.80	0.57
1	1	0	1	0	1	0	2	0	0	1	0	0.07	101.60	6.88	[14]	−1.85	1.05
1	1	0	1	0	1	0	1	0	0	0	0	0.07	105.00	6.80	[17]	1.44	0.97
1	1	0	1	0	1	0	1	0	0	0	0	0.07	102.50	5.50	[14]	−0.98	−0.33
1	1	0	1	0	1	0	2	0	0	0	0	0.14	102.10	3.70	[17]	−1.41	−1.17
1	1	0	1	0	1	0	2	0	0	0	0	0.14	103.20	4.50	[14]	−0.34	−0.37
1	1	0	1	0	1	0	3	0	0	1	0	0.14	103.70	3.80	[14]	0.14	−1.07
1	1	0	1	0	1	0	3	0	0	0	0	0.21	99.50	2.70	[14]	−3.98	−1.20
1	1	0	1	0	1	1	0	0	0	1	0	0.23	104.00	2.91	[14]	0.33	−0.72
1	1	0	1	0	1	1	0	0	0	0	0	0.30	106.10	0.90	[17]	2.25	−1.76
1	1	0	1	0	1	1	1	0	0	0	0	0.37	100.00	1.00	[14]	−3.75	−0.69

Table 2 (*continued*)

J'	K'_a	K'_c	J''	K''_a	K''_c	v'_1	v'_2	v'_3	v''_1	v''_2	v''_3	Δv	γ_{air}	δ_{air}	Ref.	%	Dif
1	1	0	1	0	1	1	2	0	0	0	0	0.44	102.20	1.42	[14]	−1.79	0.69
1	1	0	1	0	1	2	0	0	0	0	0	0.60	106.90	1.46	[14]	2.25	2.94
1	1	0	1	0	1	0	0	2	0	0	0	0.60	103.60	−0.67	[14]	−0.90	0.81
1	1	0	1	0	1	2	2	0	0	0	0	0.74	104.00	−9.00	[16]	−1.04	−5.59
1	1	0	1	0	1	3	0	0	0	0	0	0.90	105.50	−0.90	[7]	−0.33	4.72
1	1	0	1	0	1	1	0	2	0	0	0	0.90	102.00	−3.00	[16]	−3.64	2.62
1	1	0	1	0	1	1	0	2	0	0	0	0.90	106.60	−2.60	[7]	0.71	3.02
1	1	0	1	0	1	1	0	2	0	0	0	0.90	73.00		[16]	−31.03	
1	1	0	1	0	1	1	1	2	0	0	0	0.97	97.00	−4.00	[16]	−8.69	2.59
1	1	0	1	0	1	3	1	0	0	0	0	0.97	106.00	−4.00	[16]	−0.22	2.59
1	1	0	1	0	1	1	2	2	0	0	0	1.04	135.00	−32.00	[15]	26.60	−24.45
1	1	0	1	0	1	2	0	2	0	0	0	1.20	112.00	−8.00	[15]	4.02	1.76
1	1	0	1	0	1	0	0	4	0	0	0	1.20	52.00	−12.00	[15]	−51.71	−2.24
1	1	0	1	0	1	2	1	2	0	0	0	1.27	110.00	−17.00	[15]	1.68	−6.27
1	1	0	1	0	1	4	1	0	0	0	0	1.27	110.00	−11.00	[15]	1.68	−0.27
1	1	0	1	0	1	4	2	0	0	0	0	1.34	122.00	−2.00	[15]	12.23	9.69
1	1	0	1	0	1	2	2	2	0	0	0	1.34	86.00	−26.00	[15]	−20.89	−14.31
1	1	0	1	0	1	5	0	0	0	0	0	1.50	72.00	−26.00	[15]	−34.56	−12.10
1	1	0	1	0	1	3	0	2	0	0	0	1.50	111.00	−15.00	[15]	0.89	−1.10
1	1	0	1	0	1	1	0	4	0	0	0	1.50	149.00	81.00	[15]	35.42	94.90
1	1	0	1	0	1	5	1	0	0	0	0	1.57	91.00	−5.00	[15]	−17.76	9.87
1	1	0	1	0	1	6	0	0	0	0	0	1.80	110.00	−18.00	[15]	−2.57	0.04

Note: Δv is equal to $(0.3 \times (v'_1 - v''_1) + 0.07 \times (v'_2 - v''_2) + 0.3 \times (v'_3 - v''_3))$. γ_{air} and δ_{air} are, respectively, the experimental or theoretical air-broadened half-widths and air pressure-induced frequency shifts in $10^{-3}\,cm^{-1}\,atm^{-1}$, and the Ref. column contains references related to these values. When there is a blank instead of a value for γ_{air} or δ_{air}, it means that no values are given in the corresponding reference. The column noted % represents the difference in % between the experimental or theoretical air-broadened half-widths and the corresponding calculated value using the semi-empirical coefficients (see Section 4). The column noted Dif represents the difference in $10^{-3}\,cm^{-1}\,atm^{-1}$ between the experimental or theoretical air pressure-induced frequency shifts and the corresponding calculated value using the semi-empirical coefficients (see Section 4).

4.1. Semi-empirical coefficients obtained directly from the fit of the measurements and theoretical calculations

The set of experimental and theoretical data used in this work for modeling the vibrational dependence of the air-broadened half-widths and the air pressure-induced frequency shifts of the $H_2^{16}O$ isotopologue is described in Section 3 and Table 1. The first step was to sort these data by rotational quantum numbers (see Table 2), and the second step was to fit all the values of air-broadened half-widths and all the values of air pressure-induced frequency shifts with the same rotational quantum numbers and different vibrational quantum numbers to Eqs. (1) and (2), respectively.

It should be stressed that all these fits have been done individually by careful inspection of the data and graphical analysis. The reason for this approach was due to the fact that some

experimental results, mainly from Refs. [15,16], exhibited in a number of cases a large difference for both γ_{air} and δ_{air} compared with the vibrational dependence of these parameters exhibited by all the other experiments and theoretical calculations (see in Table 2 the differences between experimental or theoretical values and the corresponding values calculated using semi-empirical coefficients). It should be emphasized that these exceptions are usually for high vibrational states where the spectral signal is weak resulting in some erroneous fits. When it is possible to compare the data from Refs. [15,16] with other measurements good agreement is generally observed. The outlying values are easily detected since they are often too large or small by factors of 2 or more. For example, Ref. [15] reports the air-broadened half-width of the $1_{01} \leftarrow 0_{00}$ transition for the $2v_1 + 3v_2 + v_3$ band as $0.041\,cm^{-1}atm^{-1}$ compared with values from other measurements around $0.1\,cm^{-1}atm^{-1}$ (see Table 2). These erroneous results are easily detected by plotting all the measurements and calculations for the same set of rotational quantum numbers versus Δv. Figs. 2 and 3 show fits of the measurements and the calculations, respectively, of air-broadened half-widths and air pressure-induced frequency shifts for six different sets of rotational quantum numbers. In these two figures, a different symbol has been used for each reference to the measurements and calculations and another symbol has been used to overlay them in order to identify which data have been kept for the fit. Indeed, the advantage of doing all these fits manually is that any suspicious data can be evaluated and removed before fitting the semi-empirical coefficients.

Concerning the manual selection of the measurements and calculations, when a large number of data were available for a set of rotational quantum numbers, and when one of the values of either the air-broadened half-width or the air pressure-induced frequency shift (for the same transition and the same reference) appeared erroneous, both values of γ_{air} and δ_{air} were removed from the fits. However, when the number of data for the fit was small, we sometimes retained a value of the air-broadened half-widths (or air pressure-induced frequency shifts), whereas the value of the air pressure-induced frequency shifts (or air-broadened half-widths) for the same line was removed from the data used in the fit. This explains why some values were not retained for a fit although they were in agreement with the other references. As illustrated in Figs. 2 and 3, almost all data that were removed from the fit of the semi-empirical coefficients come from Refs. [15,16]. The research presented in the latter works encompasses the measurements of line parameters for 5000 transitions between 13,000 to $26,000\,cm^{-1}$ and 7000 transitions between 9250 to $13,000\,cm^{-1}$, respectively. The retrieval of these line parameters was performed using an automated procedure, and it is known that some measured lines were blended or too weak for an accurate analysis of the air-broadened half-widths and the air pressure-induced frequency shifts. There is an ongoing effort to assign and refine the parameters of these data [21]. While a majority of data that were eliminated from the fit of the semi-empirical coefficients come from Refs. [15,16], it should be emphasized that the majority of these data is quite good and in agreement with other

Fig. 2. Sample of fits modeling the vibrational dependence of the air-broadening half-widths for different sets of rotational quantum numbers. The measurements and calculations used in this work are represented as following: hexagons for Ref. [13], diamonds for Ref. [12], triangles for Ref. [14], upside-down triangles for Ref. [17], stars for Ref. [18], plus signs for Ref. [7], squares for Ref. [16], circles for Ref. [15]. The continuous line is the linear fit of the experimental and theoretical values retained for the fit (noted by using the cross symbol (×) in front of the previous symbols).

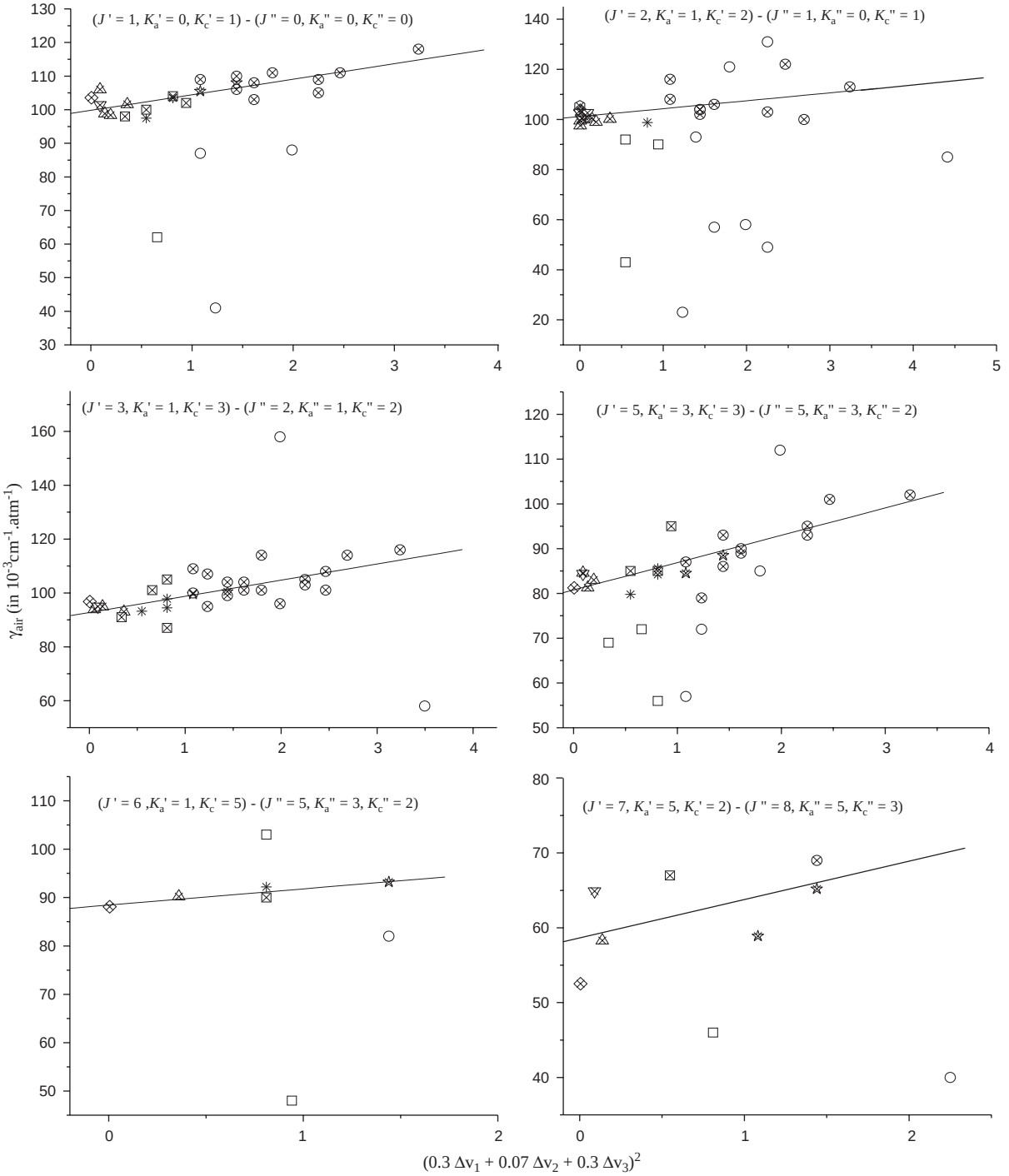
(J ' = 1, Ka' = 0, Kc' = 1) - (J " = 0, Ka" = 0, Kc" = 0)
(J ' = 2, Ka' = 1, Kc' = 2) - (J " = 1, Ka" = 0, Kc" = 1)
(J ' = 3, Ka' = 1, Kc' = 3) - (J " = 2, Ka" = 1, Kc" = 2)
(J ' = 5, Ka' = 3, Kc' = 3) - (J " = 5, Ka" = 3, Kc" = 2)
(J ' = 6 ,Ka' = 1, Kc' = 5) - (J " = 5, Ka" = 3, Kc" = 2)
(J ' = 7, Ka' = 5, Kc' = 2) - (J " = 8, Ka" = 5, Kc" = 3)
γair (in 10-3cm-1.atm-1)
(0.3 Δν1 + 0.07 Δν2 + 0.3 Δν3)2

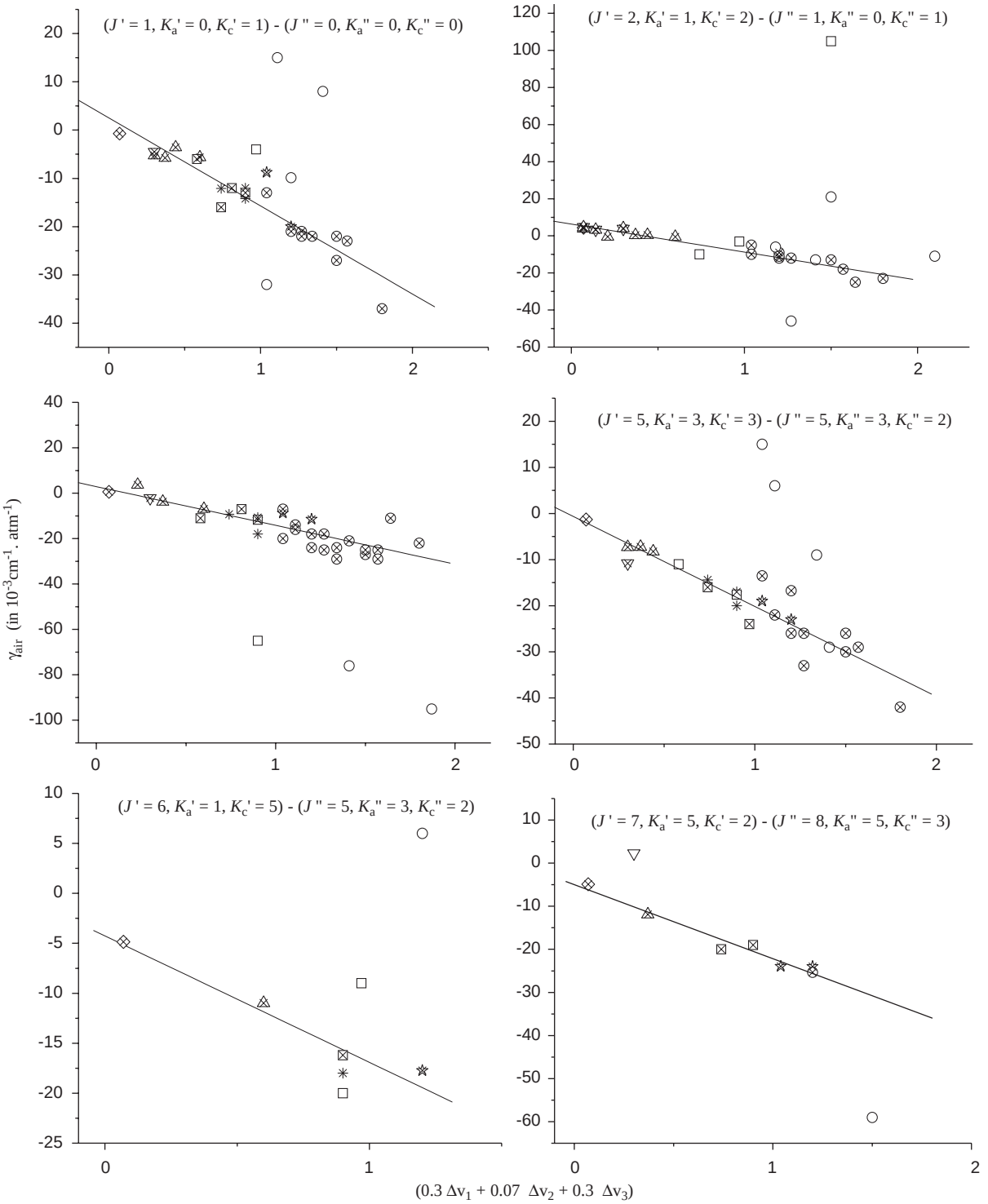

Fig. 3. Sample of fits modeling the vibrational dependence of the air pressure-induced frequency shifts for different sets of rotational quantum numbers. The definition of the symbols used in this figure is the same as in Fig. 2.

measurements and calculations. Because of the access these data provide to high vibrational levels, they were invaluable in determining the slope of the fits.

Finally, semi-empirical coefficients $\gamma^0_{f\leftarrow i}$ and $A_{f\leftarrow i}$ related to the vibrational dependence of the air-broadened half widths have been determined for 613 sets of rotational quantum numbers, and semi-empirical coefficients $\delta^0_{f\leftarrow i}$ and $B_{f\leftarrow i}$ related to the vibrational dependence of the air pressure-induced frequency shifts have been obtained for 793 sets of rotational quantum numbers. A sample of these semi-empirical coefficients obtained directly from the fits of measurements and theoretical calculations is given in Table 3 (where the statistical uncertainty of the fit is indicated for each coefficient). Note that because the fits were done manually for each set of rotational quantum numbers by removing some experimental data, the results obtained in this work are dependent on the final points chosen. However, the deletion of these data resulted in only slightly different values of the semi-empirical coefficients.

4.2. Additional approximations used to obtain a complete set of semi-empirical coefficients

The sets of semi-empirical coefficients determined in Section 4.1 are not sufficient to update γ_{air} and δ_{air} for all $H_2^{16}O$ transitions present in the *HITRAN* database [1]. Of the 4239 sets of rotational quantum numbers present in the database, the approximately 700 sets of semi-empirical coefficients obtained as described above represent, respectively, 46% and 53% of the number of air-broadened half-widths and air pressure-induced frequency shifts needed for a complete update. For this reason, different series of approximations have been performed. These approximations are prioritized into three levels.

4.2.1. First level of approximation

The first level of approximation, i.e. the higher priority situation, consisted of using average values of the semi-empirical coefficients $A_{f\leftarrow i}$ and $B_{f\leftarrow i}$, but still using observed data and theoretical calculations to determine $\gamma^0_{f\leftarrow i}$ and $\delta^0_{f\leftarrow i}$. The average values of $A_{f\leftarrow i}$ and $B_{f\leftarrow i}$, designated respectively $\tilde{A}_i$ and $\tilde{B}_i$, have been obtained by averaging all the coefficients $A_{f\leftarrow i}$ and $B_{f\leftarrow i}$ found in Section 4.1 and corresponding to the same set of lower rotational quantum numbers. The complete list of these average values is given in Table 4. The measurements and theoretical calculations used in this first level of approximation correspond to sets of rotational quantum numbers for which it was impossible to establish a vibrational dependence of either the air-broadened half-widths or the air pressure-induced frequency shifts.

In order to obtain the semi-empirical coefficients $\gamma^0_{f\leftarrow i}$ and/or $\delta^0_{f\leftarrow i}$ for a set of rotational quantum numbers, we chose one or several data from the set of measurements and theoretical calculations, which involve if possible small values of Δv. Then, using Eqs. (1) and (2) with the average values $\tilde{A}_i$ and $\tilde{B}_i$, and with the values of experimental/theoretical data $\gamma_{\text{exp or calc}}$ and $\delta_{\text{exp or calc}}$, the semi-empirical coefficients $\gamma^0_{f\leftarrow i}$ and $\delta^0_{f\leftarrow i}$ are equal, respectively, to

$$\gamma^0_{f\leftarrow i} = \gamma_{\text{exp or calc}}[(v'_1, v'_2, v'_3)f \leftarrow (v''_1, v''_2, v''_3)i] - \tilde{A}_i \times (0.3\Delta v_1 + 0.07\Delta v_2 + 0.3\Delta v_3)^2, \quad (3)$$

$$\delta^0_{f\leftarrow i} = \delta_{\text{exp or calc}}[(v'_1, v'_2, v'_3)f \leftarrow (v''_1, v''_2, v''_3)i] - \tilde{B}_i \times (0.3\Delta v_1 + 0.07\Delta v_2 + 0.3\Delta v_3). \quad (4)$$

A sample of experimental and theoretical data used to deduce the semi-empirical coefficients $\gamma^0_{f\leftarrow i}$ and $\delta^0_{f\leftarrow i}$ from Eqs. (3) and (4) is presented in Table 5. The final step of this approximation

Table 3
Sample of the semi-empirical coefficients obtained directly from the fit of measurements and theoretical calculations

J'	K'_a	K'_c	J''	K''_a	K''_c	$\gamma^0_{f\leftarrow i}$	$A_{f\leftarrow i}$	$\delta^0_{f\leftarrow i}$	$B_{f\leftarrow i}$
1	0	1	0	0	0	99.9(1.0)	4.6(0.7)	2.5(1.4)	−18.2(1.4)
1	1	1	0	0	0	101.1(0.7)	1.0(1.0)	4.4(0.7)	−14.4(1.2)
0	0	0	1	0	1	99.3(1.3)	4.7(1.1)	3.7(1.6)	−16.4(1.6)
1	1	0	1	0	1	103.5(0.6)	2.9(0.6)	6.8(0.8)	−13.8(1.0)
2	0	2	1	0	1	99.8(1.2)	2.8(0.9)	6.8(1.4)	−16.8(1.4)
2	1	2	1	0	1	101.1(1.3)	3.2(1.0)	6.3(0.8)	−15.1(0.8)
2	2	0	1	0	1	103.0(1.9)	2.9(2.1)	8.5(1.4)	−13.0(1.7)
1	0	1	1	1	0	103.6(1.0)	0.4(1.0)	−4.0(1.2)	−15.4(1.4)
1	1	1	1	1	0	101.8(1.5)	2.3(1.1)	−1.9(1.4)	−16.4(1.3)
2	1	1	1	1	0	96.0(1.6)	9.2(1.4)	0.5(2.6)	−18.4(2.5)
2	2	1	1	1	0	98.9(1.1)	2.5(1.0)	3.7(1.1)	−17.6(1.2)
0	0	0	1	1	1	102.3(0.4)	5.8(3.1)	−2.6(2.6)	−17.2(3.7)
1	1	0	1	1	1	98.0(1.4)	4.7(1.0)	6.0(1.8)	−15.7(1.7)
2	0	2	1	1	1	100.4(1.0)	3.3(1.6)	−0.2(1.0)	−13.0(1.8)
2	1	2	1	1	1	98.0(1.5)	2.3(1.2)	2.1(1.6)	−14.4(1.6)
2	2	0	1	1	1	98.0(2.4)	3.7(2.4)	8.7(1.4)	−24.0(1.7)
1	0	1	2	0	2	99.5(1.6)	6.1(1.1)	−1.5(2.3)	−15.9(2.0)
1	1	1	2	0	2	99.4(1.2)	4.3(1.8)	2.2(1.2)	−14.7(1.8)
2	1	1	2	0	2	97.6(2.7)	4.0(2.7)	8.5(5.5)	−20.6(6.1)
2	2	1	2	0	2	99.4(1.3)	2.1(1.5)	5.1(1.7)	−13.8(2.1)
3	0	3	2	0	2	97.6(1.1)	1.6(0.7)	8.5(2.2)	−20.4(1.9)
3	1	3	2	0	2	98.9(1.0)	2.6(0.8)	6.9(1.4)	−17.3(1.5)
3	2	1	2	0	2	98.2(3.7)	7.4(3.5)	6.1(3.0)	−13.6(3.3)
1	1	0	2	1	1	95.6(1.5)	7.0(1.2)	1.0(1.5)	−13.0(1.5)
2	0	2	2	1	1	101.7(1.9)	1.0(1.4)	−2.8(3.1)	−17.3(3.1)
2	1	2	2	1	1	98.2(1.3)	4.5(1.3)	0.3(1.3)	−15.7(1.5)
2	2	0	2	1	1	—(–)	—(–)	3.8(1.8)	−18.0(2.4)
3	1	2	2	1	1	91.7(1.4)	7.2(1.1)	0.1(2.1)	−17.6(2.0)
3	2	2	2	1	1	96.5(1.1)	2.4(1.1)	2.8(1.1)	−18.5(1.3)
3	3	0	2	1	1	90.5(4.6)	7.5(5.2)	4.5(2.8)	−15.9(3.3)
1	0	1	2	1	2	100.7(0.8)	5.2(0.9)	−3.5(1.2)	−16.8(1.6)
1	1	1	2	1	2	96.2(1.0)	5.2(0.7)	0.9(1.2)	−15.7(1.1)
2	1	1	2	1	2	95.8(1.6)	4.6(1.2)	4.8(2.5)	−17.0(2.4)
2	2	1	2	1	2	95.3(0.8)	5.1(0.8)	6.6(1.6)	−19.1(1.9)
3	0	3	2	1	2	92.6(1.5)	6.6(1.0)	−0.2(1.3)	−15.6(1.2)
3	1	3	2	1	2	92.7(1.6)	6.0(1.1)	2.9(2.4)	−17.0(2.1)
3	2	1	2	1	2	96.2(1.4)	3.6(1.2)	6.8(0.6)	−15.5(0.7)
3	3	1	2	1	2	94.7(0.5)	2.4(0.6)	8.8(3.0)	−17.5(3.8)
1	1	1	2	2	0	99.0(2.9)	2.4(3.6)	−4.5(2.2)	−13.4(3.2)
2	1	1	2	2	0	95.3(1.2)	3.0(1.2)	1.1(1.7)	−21.8(2.1)
2	2	1	2	2	0	89.6(2.2)	4.5(1.7)	3.0(1.5)	−18.3(1.5)
3	2	1	2	2	0	89.3(1.7)	5.2(1.4)	1.0(2.6)	−15.0(2.5)
3	3	1	2	2	0	84.1(1.9)	2.7(2.0)	2.7(3.0)	−19.1(4.0)
1	1	0	2	2	1	98.4(1.6)	3.5(1.4)	1.2(1.6)	−16.5(1.8)
2	0	2	2	2	1	99.1(2.7)	5.3(2.5)	−5.1(1.7)	−10.0(1.9)
2	1	2	2	2	1	94.9(1.9)	3.4(1.7)	−0.4(1.4)	−15.1(1.6)
2	2	0	2	2	1	88.3(1.9)	4.5(1.3)	2.0(2.2)	−18.6(2.0)

Table 3 (*continued*)

J'	K'_a	K'_c	J''	K''_a	K''_c	$\gamma^0_{f\leftarrow i}$	$A_{f\leftarrow i}$	$\delta^0_{f\leftarrow i}$	$B_{f\leftarrow i}$
3	1	2	2	2	1	94.9(2.3)	6.5(1.7)	2.0(2.2)	−18.6(2.0)
3	2	2	2	2	1	89.9(1.8)	5.1(1.3)	1.9(1.8)	−18.3(1.7)
3	3	0	2	2	1	83.7(0.8)	3.4(0.7)	4.0(0.7)	−18.7(0.8)
2	0	2	3	0	3	95.3(1.9)	6.3(1.4)	−2.8(2.2)	−17.3(1.9)
2	1	2	3	0	3	95.6(1.2)	5.2(1.0)	4.8(2.2)	−20.9(2.4)
2	2	0	3	0	3	99.7(2.0)	3.6(1.9)	9.4(7.6)	−19.7(8.2)
3	1	2	3	0	3	96.2(2.1)	7.0(2.2)	5.1(0.6)	−16.5(0.7)
3	2	2	3	0	3	94.3(1.3)	6.5(1.7)	6.3(0.9)	−17.6(1.2)
4	0	4	3	0	3	91.1(1.8)	4.6(1.3)	5.5(2.2)	−18.5(2.1)
4	1	4	3	0	3	92.8(1.1)	4.0(1.0)	6.8(1.3)	−18.1(1.5)
4	2	2	3	0	3	96.1(1.3)	4.7(0.9)	8.4(1.7)	−16.6(1.7)
4	3	2	3	0	3	94.6(1.4)	5.1(1.9)	7.7(0.8)	−13.9(1.1)

Note: In parenthesis are given the statistical uncertainty (1σ) of the fit for each parameter. The semi-empirical coefficients are given in $10^{-3}\,cm^{-1}\,atm^{-1}$.

Table 4
Average values of the semi-empirical coefficients determined for each set of lower rotational quantum numbers

J''	K''_a	K''_c	$\tilde{\gamma}^0_i$	$\tilde{A}_i$	$\tilde{\delta}^0_i$	$\tilde{B}_i$
0	0	0	100.5	2.8	3.5	−16.3
1	0	1	101.3	3.3	6.4	−15.0
1	1	0	100.1	3.6	−0.4	−16.9
1	1	1	99.3	4.0	2.8	−16.9
2	0	2	98.7	4.0	5.1	−16.6
2	1	1	95.7	4.9	1.4	−16.6
2	1	2	95.5	4.8	3.4	−16.8
2	2	0	91.5	5.6	0.7	−17.5
2	2	1	92.7	4.5	0.8	−16.5
3	0	3	95.1	5.2	5.7	−17.7
3	1	2	93.5	4.1	3.5	−15.4
3	1	3	94.3	4.3	3.5	−20.3
3	2	1	91.1	4.8	−0.2	−16.6
3	2	2	89.6	5.7	−0.1	−14.1
3	3	0	81.0	6.5	−1.7	−16.2
3	3	1	76.0	5.0	0.0	−17.7
4	0	4	88.6	4.8	4.5	−18.8
4	1	3	90.5	4.9	4.9	−17.9
4	1	4	88.5	5.8	5.1	−19.0
4	2	2	90.3	5.1	−0.7	−15.3
4	2	3	86.2	6.4	1.1	−17.1
4	3	1	80.8	7.4	−0.6	−17.1
4	3	2	82.1	4.9	−1.5	−16.4
4	4	0	50.6	3.8	−0.5	−21.7
4	4	1	69.6	7.8	−0.6	−21.3

Table 4 (*continued*)

J''	K''_a	K''_c	$\tilde{\gamma}_i^0$	$\tilde{A}_i$	$\tilde{\delta}_i^0$	$\tilde{B}_i$
5	0	5	82.4	4.8	3.3	−20.0
5	1	4	86.9	5.5	5.2	−18.9
5	1	5	80.0	6.5	1.9	−19.3
5	2	3	89.1	5.0	0.9	−18.0
5	2	4	82.1	4.9	0.8	−17.5
5	3	2	83.8	5.7	−0.2	−18.3
5	3	3	79.2	6.4	−1.2	−17.2
5	4	1	72.9	6.6	−3.4	−16.0
5	4	2	67.7	7.6	−2.5	−18.3
5	5	0	53.3	11.9	−0.5	−22.9
5	5	1	—	—	3.4	−26.2
6	0	6	69.5	8.5	2.1	−21.4
6	1	5	80.4	4.8	4.3	−20.3
6	1	6	71.1	8.4	1.8	−22.2
6	2	4	86.6	4.3	0.3	−17.6
6	2	5	76.0	6.9	1.0	−19.8
6	3	3	83.6	4.6	−0.6	−16.6
6	3	4	71.0	5.7	−0.9	−17.9
6	4	2	71.0	6.1	−1.4	−19.8
6	4	3	68.1	8.4	−2.5	−18.5
6	5	1	59.9	11.3	1.4	−22.8
6	5	2	43.9	8.5	−1.9	−22.0
6	6	1	36.6	11.8	0.7	−26.3
7	0	7	60.2	7.4	0.6	−23.2
7	1	6	74.2	6.3	5.3	−22.1
7	1	7	60.7	8.4	0.9	−24.4
7	2	5	81.7	5.3	2.1	−18.6
7	2	6	67.8	8.5	1.0	−21.3
7	3	4	85.5	5.8	0.1	−20.1
7	3	5	72.9	5.9	0.4	−18.2
7	4	3	72.8	8.9	−3.1	−17.2
7	4	4	63.3	7.2	−2.1	−17.2
7	5	2	59.4	7.7	−2.1	−23.1
7	5	3	45.7	8.4	−2.6	−19.3
7	6	1	39.9	18.9	−4.0	−18.2
7	6	2	—	—	1.3	−14.9
7	7	0	28.0	14.5	−1.1	−26.4
8	0	8	45.7	12.2	−1.4	−25.4
8	1	7	61.2	12.7	3.7	−21.8
8	1	8	50.1	10.1	−0.9	−25.1
8	2	6	64.7	5.2	4.2	−19.0
8	2	7	61.0	9.2	0.5	−24.1
8	3	5	67.7	4.0	−1.6	−15.8
8	3	6	60.9	6.2	0.1	−21.1
8	4	4	75.2	7.2	−1.9	−19.8
8	4	5	58.1	7.8	−2.1	−21.1
8	5	3	53.3	12.8	−3.9	−18.4
8	5	4	55.7	12.2	−1.6	−21.6

Table 4 (*continued*)

J''	K''_a	K''_c	$\tilde{\gamma}_i^0$	$\tilde{A}_i$	$\tilde{\delta}_i^0$	$\tilde{B}_i$
8	6	2	41.6	8.5	−1.3	−28.2
8	6	3	42.2	20.5	−2.5	−18.7
8	7	2	34.7	10.4	−3.3	−25.7
8	8	1	18.7	37.4	−2.0	−21.0
9	0	9	39.5	15.3	−0.4	−27.3
9	1	8	47.0	8.5	2.0	−25.4
9	1	9	38.7	16.2	−0.2	−26.5
9	2	7	56.8	4.0	6.2	−23.3
9	2	8	28.9	5.5	0.3	−28.1
9	3	6	62.3	6.5	−0.8	−21.2
9	3	7	58.8	7.9	−2.2	−26.4
9	4	5	57.4	4.8	−3.3	−18.8
9	4	6	62.0	11.9	−4.0	−25.4
9	5	4	58.1	15.1	−4.8	−20.1
9	5	5	50.7	6.7	−3.4	−20.1
9	6	3	46.0	12.4	−2.0	−18.2
9	6	4	—	—	−2.7	−24.9
9	7	2	34.2	8.9	−3.8	−23.1
9	8	1	28.0	8.8	−0.3	−22.5
10	0	10	24.1	11.1	−1.6	−29.8
10	1	9	33.6	10.0	0.9	−33.6
10	1	10	28.3	10.4	−1.7	−28.6
10	2	8	—	—	−2.5	−30.8
10	2	9	32.2	13.2	−0.8	−26.9
10	3	7	—	—	3.1	−20.8
10	3	8	43.2	10.3	−4.9	−24.9
10	4	6	—	—	−1.7	−22.6
10	4	7	33.0	4.5	−6.2	−25.7
10	5	6	47.7	18.6	−3.5	−21.9
10	6	4	—	—	−2.9	−26.6
10	6	5	—	—	−0.9	−32.8
11	0	11	8.6	3.0	−1.0	−33.2
11	1	10	24.8	11.9	−2.2	−31.0
11	1	11	—	—	0.0	−34.0
11	2	9	48.0	5.4	−0.4	−25.9
11	2	10	—	—	−3.1	−30.3
11	3	8	—	—	2.5	−23.8
11	3	9	—	—	1.2	−34.7
11	4	7	—	—	0.4	−27.4
11	4	8	—	—	1.1	−29.6
11	5	6	—	—	−0.9	−14.9
12	0	12	17.1	15.4	−0.5	−35.5
12	1	11	—	—	−2.1	−31.6
12	1	12	16.4	14.2	−1.8	−31.2
12	2	10	—	—	0.1	−24.8
12	2	11	—	—	−2.5	−30.6
12	3	10	12.5	10.2	0.9	−37.7
12	4	9	—	—	−1.8	−40.2

Table 4 (*continued*)

J''	K''_a	K''_c	$\tilde{\gamma}^0_i$	$\tilde{A}_i$	$\tilde{\delta}^0_i$	$\tilde{B}_i$
12	5	8	—	—	1.2	−28.8
13	0	13	—	—	−1.2	−34.0
13	1	12	7.1	4.9	−2.0	−32.9
13	1	13	—	—	−0.6	−32.4
13	2	11	—	—	−0.7	−32.6
14	1	14	6.6	6.4	−0.1	−34.2

Note: The semi-empirical coefficients are given in $10^{-3}\,cm^{-1}\,atm^{-1}$.

Table 5
Sample of experimental or theoretical data used to deduce the semi-empirical coefficients $\gamma^0_{f\leftarrow i}$ and $\delta^0_{f\leftarrow i}$ from Eqs. (1) and (2), and from an average value of the semi-empirical coefficients $A_{f\leftarrow i}$ and $B_{f\leftarrow i}$ from Table 4

J'	K'_a	K'_c	J''	K''_a	K''_c	v'_1	v'_2	v'_3	v''_1	v''_2	v''_3	γ_{air}	δ_{air}	Ref.	$\gamma^0_{f\leftarrow i}$	$\tilde{A}_i$	$\delta^0_{f\leftarrow i}$	$\tilde{B}_i$
2	1	2	1	1	0	2	2	1	0	0	0	107.50	−11.36	[18]	103.76	3.60	6.92	−16.9
2	1	2	1	1	0	3	0	1	0	0	0	108.20	−13.50	[18]	103.88	3.60	10.84	−16.9
2	2	0	2	1	1	0	1	0	0	0	0	97.48	1.18	[12]	97.14	4.90	1.26	−16.6
2	2	0	2	1	1	0	1	0	0	0	0	97.50	2.20	[14]	97.16	4.90	2.28	−16.6
2	2	0	2	1	1	0	1	0	0	0	0	97.50	2.70	[17]	97.16	4.90	2.78	−16.6
1	0	1	2	2	0	0	1	0	0	0	0	103.82	−9.54	[12]	103.43	5.60	−9.45	−17.5
1	0	1	2	2	0	0	0	1	0	0	0	102.90	−9.50	[14]	101.22	5.60	−7.92	−17.5
3	0	3	2	2	0	0	1	0	0	0	0	99.60	−6.10	[12]	99.21	5.60	−6.01	−17.5
3	0	3	2	2	0	0	0	1	0	0	0	102.00	−7.50	[14]	100.32	5.60	−5.92	−17.5
3	1	3	2	2	0	0	1	0	0	0	0	100.50	−2.65	[14]	100.11	5.60	−2.56	−17.5
3	1	3	2	2	0	0	1	0	0	0	0	99.06	−4.14	[12]	98.67	5.60	−4.05	−17.5
3	1	3	2	2	0	0	1	0	0	0	0	98.50	−1.60	[17]	98.11	5.60	−1.51	−17.5
3	3	0	3	0	3	0	1	0	0	0	0	95.33	8.23	[12]	94.97	5.20	8.32	−17.7
3	3	0	3	0	3	0	2	0	0	0	0	98.10	5.40	[14]	97.37	5.20	5.75	−17.7
4	4	0	3	1	3	0	1	0	0	0	0	92.70	5.02	[14]	92.40	4.30	5.12	−20.3
4	4	0	3	1	3	0	1	0	0	0	0	92.92	5.86	[12]	92.62	4.30	5.96	−20.3
4	1	4	3	2	1	0	1	0	0	0	0	95.68	−4.41	[12]	95.34	4.80	−4.33	−16.6
4	1	4	3	2	1	0	1	0	0	0	0	96.10	−2.15	[14]	95.76	4.80	−2.07	−16.6
4	1	4	3	2	1	0	1	0	0	0	0	94.50	−2.40	[17]	94.16	4.80	−2.32	−16.6
3	0	3	3	3	0	0	1	0	0	0	0	96.03	−9.13	[12]	95.58	6.50	−9.05	−16.2
3	0	3	3	3	0	0	1	0	0	0	0	100.00	−7.15	[14]	99.55	6.50	−7.07	−16.2
3	1	3	3	3	0	0	1	0	0	0	0	95.15	−6.99	[12]	94.70	6.50	−6.91	−16.2
3	1	3	3	3	0	1	0	1	0	0	0	95.50	−9.15	[14]	91.60	6.50	−3.32	−16.2
4	1	3	3	3	0	1	0	0	0	0	0	92.34	−10.16	[12]	90.39	6.50	−8.70	−16.2
4	1	3	3	3	0	0	1	1	0	0	0	90.00	−8.00	[14]	87.59	6.50	−5.78	−16.2
4	2	3	3	3	0	0	1	0	0	0	0	86.16	−3.60	[12]	85.70	6.50	−3.52	−16.2
4	2	3	3	3	0	0	1	0	0	0	0	89.10	−2.20	[17]	88.64	6.50	−2.12	−16.2
4	2	3	3	3	0	0	1	0	0	0	0	86.70	−3.88	[14]	86.25	6.50	−3.80	−16.2
2	0	2	3	3	1	0	1	0	0	0	0	97.10	−7.38	[14]	96.75	5.00	−7.29	−17.7
2	0	2	3	3	1	0	1	0	0	0	0	98.26	−10.46	[12]	97.91	5.00	−10.37	−17.7
2	1	2	3	3	1	0	1	0	0	0	0	95.12	−8.03	[12]	94.77	5.00	−7.94	−17.7

Table 5 (*continued*)

J'	K'_a	K'_c	J''	K''_a	K''_c	v'_1	v'_2	v'_3	v''_1	v''_2	v''_3	γ_{air}	δ_{air}	Ref.	$\gamma^0_{f\leftarrow i}$	$\tilde{A}_i$	$\delta^0_{f\leftarrow i}$	$\tilde{B}_i$
2	1	2	3	3	1	1	0	1	0	0	0	96.00	−11.84	[14]	93.00	5.00	−5.47	−17.7
3	1	2	3	3	1	0	1	0	0	0	0	91.48	−5.90	[12]	91.13	5.00	−5.81	−17.7
3	1	2	3	3	1	0	1	1	0	0	0	91.80	−9.35	[14]	89.95	5.00	−6.93	−17.7
3	2	2	3	3	1	0	1	0	0	0	0	84.80	−2.06	[14]	84.45	5.00	−1.97	−17.7
3	2	2	3	3	1	0	1	0	0	0	0	84.80	−1.90	[17]	84.45	5.00	−1.81	−17.7
3	2	2	3	3	1	0	1	0	0	0	0	85.53	−2.71	[12]	85.18	5.00	−2.62	−17.7
4	0	4	3	3	1	0	1	0	0	0	0	94.53	−7.19	[12]	94.18	5.00	−7.10	−17.7
4	1	4	3	3	1	0	0	1	0	1	0	93.68	−8.05	[12]	92.53	5.00	−7.11	−17.7
4	2	2	3	3	1	0	1	0	0	0	0	92.40	−1.50	[14]	92.05	5.00	−1.41	−17.7
4	2	2	3	3	1	0	1	0	0	0	0	88.69	−2.80	[12]	88.34	5.00	−2.71	−17.7
4	2	2	3	3	1	0	1	0	0	0	0	92.40	−1.60	[17]	92.05	5.00	−1.51	−17.7
3	2	1	4	0	4	0	1	0	0	0	0	95.57	3.71	[12]	95.23	4.80	3.80	−18.8
3	3	1	4	0	4	0	1	0	0	0	0	93.75	5.64	[12]	93.41	4.80	5.73	−18.8
4	1	3	4	0	4	0	1	0	0	0	0	93.60	3.20	[14]	93.26	4.80	3.29	−18.8
4	1	3	4	0	4	0	1	0	0	0	0	92.70	2.70	[17]	92.36	4.80	2.79	−18.8
4	1	3	4	0	4	0	1	0	0	0	0	94.25	0.58	[12]	93.91	4.80	0.67	−18.8
4	3	1	4	0	4	0	1	0	0	0	0	93.30	4.90	[14]	92.96	4.80	4.99	−18.8
4	3	1	4	0	4	0	1	0	0	0	0	92.03	6.12	[12]	91.69	4.80	6.21	−18.8
5	4	1	4	0	4	0	0	1	0	0	0	90.70	1.82	[14]	89.26	4.80	3.51	−18.8

Note: The semi-empirical coefficients are given in $10^{-3}\,cm^{-1}\,atm^{-1}$.

concerns the average of the semi-empirical coefficients $\gamma^0_{f\leftarrow i}$ and $\delta^0_{f\leftarrow i}$ obtained using different experimental or theoretical data but corresponding to identical sets of rotational quantum numbers. A sample of the results of these averages is given in Table 6. With this first-level approximation, we obtained semi-empirical coefficients describing the air-broadened half-widths for 1571 sets of rotational quantum numbers, and semi-empirical coefficients describing the air pressure-induced frequency shifts for 2124 sets of rotational quantum numbers.

4.2.2. Second level of approximation

The principle of the second level of approximation is similar to that of the first level. This approximation is for cases where we could not determine the average values of $A_{f\leftarrow i}$ and $B_{f\leftarrow i}$ in Eqs. (3) and (4) for certain sets of rotational quantum numbers corresponding to the experimental and theoretical data. Indeed, for these sets of rotational quantum numbers, no vibrational dependence was obtained from the observations and theoretical calculations. In order to determine the semi-empirical coefficients $\gamma^0_{f\leftarrow i}$ and $\delta^0_{f\leftarrow i}$ for these sets of rotational quantum numbers, we considered $\tilde{A}_i$ and $\tilde{B}_i$ found in Table 4 as a function of $J''(J''+1)+K''_a-K''_c+1$ (a unique energy-ordered rotational state index for asymmetric rotors) and used extrapolation. The plots of these extrapolations are presented in Figs. 4 and 5. A linear fit was used to reproduce the rotational dependence of $\tilde{A}_i$ and $\tilde{B}_i$. However, when $J''(J''+1)+K''_a-K''_c+1\geqslant 200$, the extrapolation was no longer used and the $\tilde{A}_i$ and $\tilde{B}_i$ coefficients were fixed to 0.0133 and $-0.0356\,cm^{-1}\,atm^{-1}$, respectively.

Table 6
Sample of average values of semi-empirical coefficients obtained for each set of rotational quantum numbers from experimental or theoretical data of Table 5

J'	K'_a	K'_c	J''	K''_a	K''_c	$\tilde{\gamma}^0_{f\leftarrow i}$	$\tilde{A}_i$	$\tilde{\delta}^0_{f\leftarrow i}$	$\tilde{B}_i$
2	1	2	1	1	0	103.8	3.6	8.9	−16.9
2	2	0	2	1	1	97.2	4.9	2.1	−16.6
1	0	1	2	2	0	102.3	5.6	−8.7	−17.5
3	0	3	2	2	0	99.8	5.6	−6.0	−17.5
3	1	3	2	2	0	99.0	5.6	−2.7	−17.5
3	3	0	3	0	3	96.2	5.2	7.0	−17.7
4	4	0	3	1	3	92.5	4.3	5.5	−20.3
4	1	4	3	2	1	95.1	4.8	−2.9	−16.6
3	0	3	3	3	0	97.6	6.5	−8.1	−16.2
3	1	3	3	3	0	93.2	6.5	−5.1	−16.2
4	1	3	3	3	0	89.0	6.5	−7.2	−16.2
4	2	3	3	3	0	86.9	6.5	−3.1	−16.2
2	0	2	3	3	1	97.3	5.0	−8.8	−17.7
2	1	2	3	3	1	93.9	5.0	−6.7	−17.7
3	1	2	3	3	1	90.5	5.0	−6.4	−17.7
3	2	2	3	3	1	84.7	5.0	−2.1	−17.7
4	0	4	3	3	1	94.2	5.0	−7.1	−17.7
4	1	4	3	3	1	92.5	5.0	−7.1	−17.7
4	2	2	3	3	1	90.8	5.0	−1.9	−17.7
3	2	1	4	0	4	95.2	4.8	3.8	−18.8
3	3	1	4	0	4	93.4	4.8	5.7	−18.8
4	1	3	4	0	4	93.2	4.8	2.2	−18.8
4	3	1	4	0	4	92.3	4.8	5.6	−18.8
5	4	1	4	0	4	89.3	4.8	3.5	−18.8
5	5	1	4	0	4	91.1	4.8	5.6	−18.8
3	3	0	4	1	3	90.3	4.9	6.3	−17.9
4	0	4	4	1	3	94.1	4.9	−1.3	−17.9
4	4	0	4	1	3	88.1	4.9	5.8	−17.9
4	3	1	4	1	4	88.8	5.8	5.2	−19.0
4	4	1	4	1	4	88.9	5.8	5.1	−19.0
5	4	1	4	1	4	88.3	5.8	5.2	−19.0
4	3	1	4	2	2	87.9	5.1	0.8	−15.3
4	4	1	4	2	2	85.1	5.1	−0.4	−15.3
5	0	5	4	2	2	93.0	5.1	−4.0	−15.3
5	1	5	4	2	2	92.3	5.1	−2.0	−15.3
5	5	1	4	2	2	83.3	5.1	1.0	−15.3
3	3	0	4	2	3	86.5	6.4	3.1	−17.1
4	4	0	4	2	3	82.8	6.4	0.6	−17.1
5	3	2	4	2	3	83.3	6.4	3.1	−17.1
5	5	0	4	2	3	82.7	6.4	2.0	−17.1
3	2	2	4	3	1	82.9	7.4	−3.0	−17.1
4	0	4	4	3	1	92.4	7.4	−6.9	−17.1
4	1	4	4	3	1	91.5	7.4	−6.5	−17.1
5	1	4	4	3	1	89.1	7.4	−5.9	−17.1
5	2	4	4	3	1	83.4	7.4	−4.8	−17.1
5	5	0	4	3	1	74.4	7.4	−3.7	−17.1

Table 6 (*continued*)

J'	K'_a	K'_c	J''	K''_a	K''_c	$\tilde{\gamma}^0_{f\leftarrow i}$	$\tilde{A}_i$	$\tilde{\delta}^0_{f\leftarrow i}$	$\tilde{B}_i$
5	0	5	4	3	2	88.5	4.9	−6.7	−16.4
5	1	5	4	3	2	87.6	4.9	−7.5	−16.4
3	1	3	4	4	0	91.9	3.8	−6.7	−21.7
3	2	1	4	4	0	83.7	3.8	−3.3	−21.7
3	3	1	4	4	0	65.5	3.8	−0.2	−21.7
4	1	3	4	4	0	88.0	3.8	−7.1	−21.7
4	2	3	4	4	0	84.1	3.8	−5.4	−21.7
5	1	5	4	4	0	88.5	3.8	−5.5	−21.7
5	3	3	4	4	0	75.0	3.8	−1.1	−21.7
3	1	2	4	4	1	89.1	7.8	−6.3	−21.3
4	1	4	4	4	1	91.0	7.8	−6.0	−21.3
5	1	4	4	4	1	86.9	7.8	−6.0	−21.3
5	2	4	4	4	1	81.0	7.8	−5.2	−21.3
5	3	2	4	4	1	80.1	7.8	−0.3	−21.3
4	2	2	5	0	5	92.5	4.8	2.4	−20.0
4	3	2	5	0	5	87.8	4.8	5.1	−20.0

Note: The semi-empirical coefficients are given in $10^{-3}\,\mathrm{cm}^{-1}\,\mathrm{atm}^{-1}$.

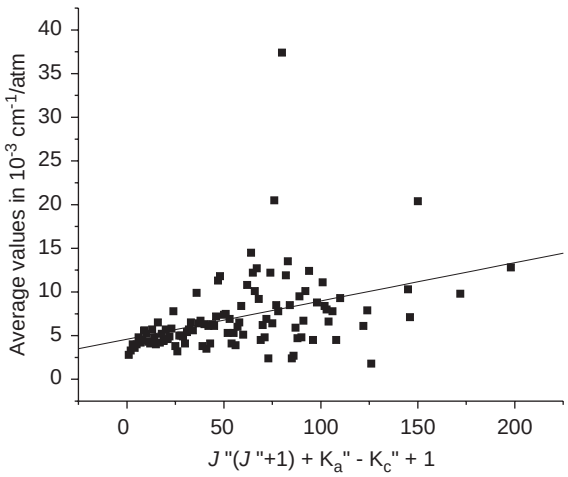

Fig. 4. Linear fit of the average values of the semi-empirical coefficients $A_{f\leftarrow i}$ obtained for identical lower-state rotational quantum numbers (see Table 4).

Using these extrapolated coefficients for $\tilde{A}_i$ and $\tilde{B}_i$, it was possible to deduce the semi-empirical coefficients $\gamma^0_{f\leftarrow i}$ and $\delta^0_{f\leftarrow i}$ from the experimental/theoretical data for which the values of $\tilde{A}_i$ and $\tilde{B}_i$ could not be obtained from the fits described in Section 4.2.1. A sample of experimental and theoretical data used to deduce the semi-empirical coefficients $\gamma^0_{f\leftarrow i}$ and $\delta^0_{f\leftarrow i}$ from Eqs. (3) and (4) is presented in Table 7. The final step of this second-level approximation concerns the average of

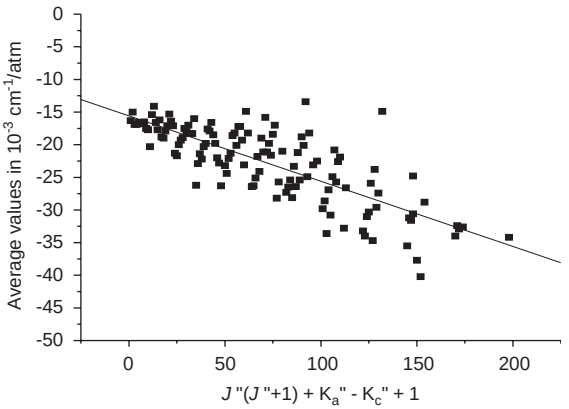

Fig. 5. Linear fit of the average values of the semi-empirical coefficients $B_{f\leftarrow i}$ obtained for identical lower-state rotational quantum numbers (see Table 4).

Table 7
Sample of experimental or theoretical data used to deduce the semi-empirical coefficients $\gamma^0_{f\leftarrow i}$ and $\delta^0_{f\leftarrow i}$ from Eqs. (1) and (2), and from average values of $A_{f\leftarrow i}$ and $B_{f\leftarrow i}$ deduced from the extrapolation of the average values of Table 4 (see Figs. 3 and 4)

J'	K'_a	K'_c	J''	K''_a	K''_c	v'_1	v'_2	v'_3	v''_1	v''_2	v''_3	γ_{air}	δ_{air}	Ref.	$\gamma^0_{f\leftarrow i}$	$\tilde{A}_i$	$\delta^0_{f\leftarrow i}$	$\tilde{B}_i$
4	0	4	5	5	1	0	1	0	0	0	0	91.91	−7.49	[12]	91.49	6.03		
4	2	2	5	5	1	0	1	0	0	0	0	85.20	−3.00	[14]	84.78	6.03		
4	2	2	5	5	1	0	1	0	0	0	0	84.14	−3.24	[12]	83.72	6.03		
4	4	0	5	5	1	0	1	0	0	0	0	48.04	−1.47	[12]	47.62	6.03		
4	4	0	5	5	1	0	1	0	0	0	0	52.50	1.80	[14]	52.08	6.03		
4	4	0	5	5	1	0	1	0	0	0	0	51.50	0.80	[17]	51.08	6.03		
5	2	4	5	5	1	0	1	0	0	0	0	80.19	−4.16	[12]	79.77	6.03		
5	3	2	5	5	1	0	0	1	0	1	0	79.13	−4.54	[12]	77.74	6.03		
5	4	2	5	5	1	0	1	0	0	0	0	59.80	3.35	[12]	59.38	6.03		
5	4	2	5	5	1	0	1	0	0	0	0	60.50	2.10	[17]	60.08	6.03		
5	4	2	5	5	1	0	1	0	0	0	0	63.70	4.50	[14]	63.28	6.03		
5	5	0	5	5	1	0	1	0	0	0	0	43.34	−3.89	[12]	42.92	6.03		
6	0	6	5	5	1	0	1	0	0	0	0	85.18	−4.41	[12]	84.76	6.03		
6	2	4	5	5	1	0	1	0	0	0	0	85.01	−2.92	[12]	84.59	6.03		
6	4	2	5	5	1	0	1	0	0	0	0	67.20	2.57	[14]	66.78	6.03		
6	4	2	5	5	1	0	1	0	0	0	0	65.80	3.59	[12]	65.38	6.03		
6	5	2	5	5	1	0	1	0	0	0	0	49.57	2.97	[12]	49.15	6.03		
6	6	0	5	5	1	0	1	0	0	0	0	36.45	−5.41	[12]	36.03	6.03		
6	6	0	5	5	1	0	2	0	0	1	0	41.30	−9.60	[14]	40.88	6.03		
5	3	3	6	6	0	0	1	0	0	0	0	72.62	0.57	[12]	72.15	6.65	0.67	−20.50
5	4	1	6	6	0	0	0	1	0	0	0	68.80	−1.40	[14]	66.81	6.65	0.45	−20.50
5	5	1	6	6	0	0	1	0	0	0	0	40.20	−3.27	[14]	39.73	6.65	−3.17	−20.50
5	5	1	6	6	0	0	1	0	0	0	0	34.66	−2.77	[12]	34.19	6.65	−2.67	−20.50
6	1	5	6	6	0	0	1	0	0	0	0	83.32	−4.19	[12]	82.85	6.65	−4.09	−20.50

Table 7 (*continued*)

J'	K'_a	K'_c	J''	K''_a	K''_c	v'_1	v'_2	v'_3	v''_1	v''_2	v''_3	γ_{air}	δ_{air}	Ref.	$\gamma^0_{f\leftarrow i}$	$\tilde{A}_i$	$\delta^0_{f\leftarrow i}$	$\tilde{B}_i$
6	3	3	6	6	0	0	1	0	0	0	0	79.99	−1.36	[12]	79.52	6.65	−1.26	−20.50
6	5	1	6	6	0	0	1	0	0	0	0	47.75	4.90	[12]	47.28	6.65	5.00	−20.50
6	5	1	6	6	0	0	1	0	0	0	0	52.20	3.46	[14]	51.73	6.65	3.56	−20.50
6	6	1	6	6	0	0	1	0	0	0	0	32.27	−4.08	[12]	31.80	6.65	−3.98	−20.50
7	3	5	6	6	0	0	1	0	0	0	0	72.34	−1.29	[12]	71.87	6.65	−1.19	−20.50
7	5	3	6	6	0	0	1	0	0	0	0	53.32	4.86	[12]	52.85	6.65	4.96	−20.50
7	5	3	6	6	0	0	1	0	0	0	0	56.10	3.07	[14]	55.63	6.65	3.17	−20.50
7	6	1	6	6	0	0	1	0	0	0	0	38.74	4.50	[12]	38.27	6.65	4.60	−20.50
7	7	1	6	6	0	0	1	0	0	0	0	26.07	−2.88	[12]	25.60	6.65	−2.78	−20.50
6	1	5	7	6	2	0	1	0	0	0	0	79.79	−6.15	[12]	79.29	7.17		
6	2	5	7	6	2	0	0	1	0	0	0	75.70	−9.09	[12]	73.55	7.17		
6	3	3	7	6	2	0	1	0	0	0	0	77.25	−1.74	[12]	76.75	7.17		
6	3	3	7	6	2	0	1	0	0	0	0	73.00	−0.85	[14]	72.50	7.17		
6	5	1	7	6	2	0	1	0	0	0	0	42.64	−0.73	[12]	42.14	7.17		
6	5	1	7	6	2	0	2	0	0	1	0	40.00	0.00	[14]	39.50	7.17		
6	5	1	7	6	2	0	1	0	0	0	0	45.20	2.40	[14]	44.70	7.17		
6	5	1	7	6	2	0	1	0	0	0	0	42.10	1.30	[17]	41.60	7.17		
6	6	1	7	6	2	0	1	0	0	0	0	39.99	−11.30	[12]	39.49	7.17		
7	3	5	7	6	2	0	1	0	0	0	0	65.71	−2.97	[12]	65.21	7.17		
7	5	3	7	6	2	0	1	0	0	0	0	49.20	3.07	[14]	48.70	7.17		
7	5	3	7	6	2	0	1	0	0	0	0	45.37	0.53	[12]	44.87	7.17		
7	6	1	7	6	2	0	1	0	0	0	0	37.30	−3.40	[12]	36.80	7.17		
7	7	1	7	6	2	0	1	0	0	0	0	39.58	−10.26	[12]	39.08	7.17		
8	3	5	7	6	2	0	1	0	0	0	0	80.06	−0.80	[12]	79.56	7.17		
8	5	3	7	6	2	0	1	0	0	0	0	57.80	0.71	[14]	57.30	7.17		
8	5	3	7	6	2	0	1	0	0	0	0	50.25	1.62	[12]	49.75	7.17		
8	6	3	7	6	2	0	1	0	0	0	0	38.88	−1.43	[12]	38.38	7.17		
8	7	1	7	6	2	0	1	0	0	0	0	33.73	−4.43	[12]	33.23	7.17		
6	3	4	7	7	1	0	0	1	0	0	0	76.76	−5.22	[12]	74.58	7.26	−3.25	−21.90
6	4	2	7	7	1	0	1	0	0	0	0	64.97	4.33	[12]	64.46	7.26	4.44	−21.90
6	5	2	7	7	1	0	0	1	0	0	0	54.00	1.80	[14]	51.82	7.26	3.77	−21.90
6	6	0	7	7	1	0	1	0	0	0	0	25.28	−5.08	[12]	24.77	7.26	−4.97	−21.90
7	4	4	7	7	1	0	1	0	0	0	0	65.68	2.45	[12]	65.17	7.26	2.56	−21.90
7	6	2	7	7	1	0	1	0	0	0	0	37.76	4.46	[12]	37.25	7.26	4.57	−21.90

Note: The semi-empirical coefficients are given in $10^{-3}\,cm^{-1}\,atm^{-1}$. A blank means that the semi-empirical coefficients have been determined from Eqs. (3) and (4) using average values of $A_{f\leftarrow i}$ and $B_{f\leftarrow i}$, and not an extrapolation of these values.

the semi-empirical coefficients $\gamma^0_{f\leftarrow i}$ and $\delta^0_{f\leftarrow i}$ obtained using different experimental or theoretical data corresponding to identical sets of rotational quantum numbers. A sample of the results of these averages is given in Table 8. With this second-level approximation, we obtained semi-empirical coefficients describing the air-broadened half-widths for 2157 sets of rotational quantum numbers, and semi-empirical coefficients describing the air pressure-induced frequency shifts for 1604 sets of rotational quantum numbers.

Table 8
Sample of average values of semi-empirical coefficients obtained for each set of rotational quantum numbers from experimental or theoretical data of Table 7

J'	K'_a	K'_c	J''	K''_a	K''_c	$\tilde{\gamma}^0_{f\leftarrow i}$	$\tilde{A}_i$	$\tilde{\delta}^0_{f\leftarrow i}$	$\tilde{B}_i$
4	0	4	5	5	1	91.5	6.0	—	—
4	2	2	5	5	1	84.2	6.0	—	—
4	4	0	5	5	1	50.3	6.0	—	—
5	2	4	5	5	1	79.8	6.0	—	—
5	3	2	5	5	1	77.7	6.0	—	—
5	4	2	5	5	1	60.9	6.0	—	—
5	5	0	5	5	1	42.9	6.0	—	—
6	0	6	5	5	1	84.8	6.0	—	—
6	2	4	5	5	1	84.6	6.0	—	—
6	4	2	5	5	1	66.1	6.0	—	—
6	5	2	5	5	1	49.1	6.0	—	—
6	6	0	5	5	1	38.5	6.0	—	—
5	3	3	6	6	0	72.2	6.7	0.7	−20.5
5	4	1	6	6	0	66.8	6.7	0.5	−20.5
5	5	1	6	6	0	37.0	6.7	−2.9	−20.5
6	1	5	6	6	0	82.8	6.7	−4.1	−20.5
6	3	3	6	6	0	79.5	6.7	−1.3	−20.5
6	5	1	6	6	0	49.5	6.7	4.3	−20.5
6	6	1	6	6	0	31.8	6.7	−4.0	−20.5
7	3	5	6	6	0	71.9	6.7	−1.2	−20.5
7	5	3	6	6	0	54.2	6.7	4.1	−20.5
7	6	1	6	6	0	38.3	6.7	4.6	−20.5
7	7	1	6	6	0	25.6	6.7	−2.8	−20.5
6	1	5	7	6	2	79.3	7.2	—	—
6	2	5	7	6	2	73.5	7.2	—	—
6	3	3	7	6	2	74.6	7.2	—	—
6	5	1	7	6	2	42.0	7.2	—	—
6	6	1	7	6	2	39.5	7.2	—	—
7	3	5	7	6	2	65.2	7.2	—	—
7	5	3	7	6	2	46.8	7.2	—	—
7	6	1	7	6	2	36.8	7.2	—	—
7	7	1	7	6	2	39.1	7.2	—	—
8	3	5	7	6	2	79.6	7.2	—	—
8	5	3	7	6	2	53.5	7.2	—	—
8	6	3	7	6	2	38.4	7.2	—	—
8	7	1	7	6	2	33.2	7.2	—	—
6	3	4	7	7	1	74.6	7.3	−3.2	−21.9
6	4	2	7	7	1	64.5	7.3	4.4	−21.9
6	5	2	7	7	1	51.8	7.3	3.8	−21.9
6	6	0	7	7	1	24.8	7.3	−5.0	−21.9
7	4	4	7	7	1	65.2	7.3	2.6	−21.9
7	6	2	7	7	1	37.2	7.3	4.6	−21.9
7	7	0	7	7	1	23.7	7.3	−3.5	−21.9
8	6	2	7	7	1	44.5	7.3	5.1	−21.9
8	7	2	7	7	1	30.3	7.3	4.7	−21.9
8	8	0	7	7	1	18.7	7.3	−1.6	−21.9

Table 8 (*continued*)

J'	K'_a	K'_c	J''	K''_a	K''_c	$\tilde{\gamma}^0_{f\leftarrow i}$	$\tilde{A}_i$	$\tilde{\delta}^0_{f\leftarrow i}$	$\tilde{B}_i$
7	3	4	8	7	1	77.7	8.0	−4.5	−23.5
7	4	4	8	7	1	57.2	8.0	1.4	−23.5
7	5	2	8	7	1	54.7	8.0	2.2	−23.5
7	6	2	8	7	1	31.6	8.0	−2.0	−23.5
7	7	0	8	7	1	30.9	8.0	−11.0	−23.5
8	4	4	8	7	1	68.1	8.0	2.9	−23.5
8	6	2	8	7	1	35.7	8.0	0.3	−23.5
8	7	2	8	7	1	28.3	8.0	−3.3	−23.5
8	8	0	8	7	1	31.2	8.0	−9.5	−23.5
9	6	4	8	7	1	40.6	8.0	1.2	−23.5

Note: The semi-empirical coefficients are given in $10^{-3}\,cm^{-1}\,atm^{-1}$.

4.2.3. Third level of approximation

Up to this point we had at our disposal measurements or theoretical calculations with which to determine the semi-empirical coefficients for the air-broadened half-widths or the air pressure-induced frequency shifts. It was also necessary to obtain semi-empirical coefficients for sets of rotational quantum numbers for which we have no measurements or calculations. For these cases, we used average values of semi-empirical coefficients obtained for either the same set of lower rotational quantum numbers or the same J quantum number. The method consists of first using the average values of the semi-empirical coefficients determined directly from the fit of the experimental or theoretical data (see Section 4.1) corresponding to identical lower rotational quantum numbers. These average values are given in Table 4. If the lower rotational quantum numbers of the transition are not present in Table 4, we used the average values of the semi-empirical coefficients determined in Section 4.2.2 (see Table 8). These coefficients are given in Table 9. Finally, if the lower rotational quantum numbers of the transition do not correspond to any case that we have treated, a rough approximation based only on the quantum number J of the lower state is used. Because of the uncertainty in this last approximation, it has only been applied to the air-broadened half-widths in order to determine a complete set of data for this parameter. In this approximation, the semi-empirical coefficients for the air-broadened half-widths are obtained by a linear fit of the average values of Table 4 versus the rotational-state index (see Fig. 4). The results are given in Table 10. Note that while this last approximation is not as accurate as the previous ones, it has only been applied to some transitions with high rotational quantum numbers.

5. Comparison with measurement and theory

In this Section, the air-broadened half-widths and air pressure-induced line shifts calculated using the empirical coefficients determined by several levels of approximation are compared with a database of measurements [22]. This database contains measurements of 14,341 transitions of

Table 9
Average values of semi-empirical coefficients on each set of lower rotational quantum numbers using the data obtained in Section 4.2.2

J''	K''_a	K''_c	$\tilde{\gamma}^0_{f\leftarrow i}$	$\tilde{A}_{f\leftarrow i}$	$\tilde{\delta}^0_{f\leftarrow i}$	$\tilde{B}_{f\leftarrow i}$	J''	K''_a	K''_c	$\tilde{\gamma}^0_i$	$\tilde{A}_i$	$\tilde{\delta}^0_i$	$\tilde{B}_i$
5	5	1	67.5	6.0			14	7	8	32.4	13.3	−4.6	−35.6
6	6	0	55.4	6.7	−0.2	−20.5	14	8	6	24.2	13.3	−4.2	−35.6
7	6	2	54.0	7.2			14	8	7	24.2	13.3	−3.5	−35.6
7	7	1	43.5	7.3	1.2	−21.9	14	9	5	21.3	13.3	−3.1	−35.6
8	7	1	42.7	8.0	−2.3	−23.5	14	9	6	22.2	13.3	−2.8	−35.6
8	8	0	27.9	8.1	0.7	−23.7	14	10	4	18.3	13.3	−3.0	−35.6
9	6	4	50.2	8.6			14	10	5	18.3	13.3	−3.0	−35.6
9	7	3	43.1	8.7	−2.9	−25.1	14	11	3	12.8	13.3	−0.5	−35.6
9	8	2	29.6	8.8	−2.9	−25.3	14	11	4	16.0	13.3	−2.5	−35.6
9	9	0	24.3	8.9	−1.6	−25.6	14	12	2	6.6	13.3	−3.0	−35.6
9	9	1	20.8	8.8	−1.1	−25.5	14	12	3	12.7	13.3	−6.1	−35.6
10	2	8	58.6	9.1			14	13	1	3.2	13.3	−1.1	−35.6
10	3	7	70.6	9.2			14	13	2	3.2	13.3	−1.1	−35.6
10	4	6	75.8	9.3			14	14	0	2.3	13.3	0.6	−35.6
10	5	5	62.5	9.4	−9.1	−26.7	14	14	1	2.3	13.3	0.6	−35.6
10	6	4	48.8	9.4			15	0	15	22.8	13.3	−2.2	−35.6
10	6	5	49.0	9.4			15	1	14	23.0	13.3	−1.3	−35.6
10	7	3	42.0	9.5	−3.1	−27.1	15	1	15	18.6	13.3	−3.7	−35.6
10	7	4	44.1	9.5	−4.0	−27.0	15	2	13	20.4	13.3	0.0	−35.6
10	8	2	32.1	9.6	−3.1	−27.3	15	2	14	19.0	13.3	−2.4	−35.6
10	8	3	32.5	9.6	−4.2	−27.2	15	3	12	26.5	13.3	2.8	−35.6
10	9	1	22.8	9.7	−5.4	−27.5	15	3	13	23.8	13.3	−0.9	−35.6
10	9	2	28.1	9.7	−4.0	−27.4	15	4	11	46.0	13.3	9.7	−35.6
10	10	0	17.1	9.8	−5.5	−27.7	15	4	12	30.5	13.3	0.2	−35.6
10	10	1	17.7	9.8	−5.1	−27.6	15	5	10	55.7	13.3	−1.6	−35.6
11	1	11	39.2	9.9			15	5	11	33.3	13.3	0.6	−35.6
11	2	10	39.9	10.0			15	6	9	54.1	13.3	−13.7	−35.6
11	3	8	65.2	10.1			15	6	10	34.6	13.3	−2.8	−35.6
11	3	9	45.3	10.1			15	7	8	32.1	13.3	−8.7	−35.6
11	4	7	72.7	10.2			15	7	9	30.6	13.3	1.6	−35.6
11	4	8	49.6	10.2			15	8	7	22.6	13.3	−3.3	−35.6
11	5	6	64.3	10.3			15	8	8	21.7	13.3	−2.2	−35.6
11	5	7	50.3	10.2	−7.1	−28.7	15	9	6	20.1	13.3	−2.8	−35.6
11	6	5	46.2	10.4	−9.0	−29.0	15	9	7	20.0	13.3	−2.8	−35.6
11	6	6	44.9	10.3	−6.5	−28.9	15	10	5	17.5	13.3	−2.7	−35.6
11	7	4	40.8	10.5	−3.6	−29.2	15	10	6	15.8	13.3	−1.5	−35.6
11	7	5	37.2	10.4	−3.1	−29.1	15	11	4	12.0	13.3	2.8	−35.6
11	8	3	32.6	10.5	−4.2	−29.4	15	11	5	12.0	13.3	2.8	−35.6
11	8	4	31.1	10.5	−4.8	−29.3	15	12	3	7.0	13.3	−2.4	−35.6
11	9	2	26.4	10.6	−6.1	−29.6	15	12	4	7.0	13.3	−2.4	−35.6
11	9	3	24.1	10.6	−7.0	−29.5	15	13	2	2.9	13.3	−2.3	−35.6
11	10	1	19.2	10.7	−4.2	−29.8	16	0	16	15.4	13.3	−1.5	−35.6
11	10	2	18.1	10.7	−3.8	−29.7	16	1	15	16.7	13.3	−2.3	−35.6
11	11	0	14.6	10.8	−0.5	−30.0	16	1	16	15.7	13.3	−3.6	−35.6
11	11	1	12.4	10.8	0.9	−29.9	16	2	14	16.0	13.3	−1.0	−35.6

Table 9 (*continued*)

J''	K''_a	K''_c	$\tilde{\gamma}^0_{f\leftarrow i}$	$\tilde{A}_{f\leftarrow i}$	$\tilde{\delta}^0_{f\leftarrow i}$	$\tilde{B}_{f\leftarrow i}$	J''	K''_a	K''_c	$\tilde{\gamma}^0_i$	$\tilde{A}_i$	$\tilde{\delta}^0_i$	$\tilde{B}_i$
12	1	11	36.6	10.9			16	2	15	16.3	13.3	−3.6	−35.6
12	2	10	38.0	11.0			16	3	13	21.5	13.3	0.6	−35.6
12	2	11	35.4	11.0			16	3	14	21.4	13.3	−1.0	−35.6
12	3	9	55.4	11.1	8.3	−30.7	16	4	12	34.5	13.3	9.5	−35.6
12	4	8	65.7	11.2	−1.9	−30.9	16	4	13	24.4	13.3	−0.1	−35.6
12	4	9	44.5	11.2			16	5	11	49.4	13.3	5.2	−35.6
12	5	7	65.6	11.3	−8.8	−31.1	16	5	12	29.0	13.3	−0.5	−35.6
12	5	8	44.9	11.2			16	6	10	56.3	13.3	−13.2	−35.6
12	6	6	46.5	11.4	−10.9	−31.3	16	6	11	31.6	13.3	−1.8	−35.6
12	6	7	42.4	11.3	−7.4	−31.2	16	7	9	35.7	13.3	−8.6	−35.6
12	7	5	36.7	11.5	−5.2	−31.5	16	7	10	26.3	13.3	−0.3	−35.6
12	7	6	36.5	11.4	−4.9	−31.4	16	8	8	18.7	13.3	−4.1	−35.6
12	8	4	30.1	11.6	−4.9	−31.7	16	8	9	20.4	13.3	−1.1	−35.6
12	8	5	31.3	11.5	−4.5	−31.6	16	9	7	16.4	13.3	−1.6	−35.6
12	9	3	23.9	11.6	−4.4	−31.9	16	9	8	16.4	13.3	−1.6	−35.6
12	9	4	24.3	11.6	−4.1	−31.8	16	10	6	15.3	13.3	−1.6	−35.6
12	10	2	18.6	11.7	−3.4	−32.1	16	10	7	15.3	13.3	−1.6	−35.6
12	10	3	18.9	11.7	−4.4	−32.0	16	11	5	12.6	13.3	2.8	−35.6
12	11	1	12.0	11.8	−2.1	−32.3	16	11	6	12.6	13.3	2.8	−35.6
12	11	2	12.0	11.8	−2.1	−32.2	16	12	5	7.6	13.3	−2.0	−35.6
12	12	0	4.7	11.9	−1.1	−32.5	17	0	17	9.6	13.3	−3.8	−35.6
12	12	1	7.7	11.9	0.6	−32.4	17	1	16	17.2	13.3	−1.3	−35.6
13	0	13	32.3	11.9			17	1	17	11.7	13.3	−1.3	−35.6
13	2	11	31.6	12.1			17	2	15	18.7	13.3	−1.1	−35.6
13	2	12	30.7	12.1	−1.1	−32.9	17	2	16	11.0	13.3	−2.2	−35.6
13	3	10	43.9	12.2	7.8	−33.2	17	3	14	18.3	13.3	0.7	−35.6
13	3	11	33.0	12.2	−2.4	−33.1	17	3	15	17.4	13.3	0.8	−35.6
13	4	9	59.0	12.3	3.3	−33.4	17	4	13	28.3	13.3	6.0	−35.6
13	4	10	37.9	12.2	−1.3	−33.3	17	4	14	24.9	13.3	−1.2	−35.6
13	5	8	66.0	12.4	−8.3	−33.6	17	5	12	47.6	13.3	11.4	−35.6
13	5	9	39.4	12.3	−4.9	−33.5	17	5	13	29.2	13.3	5.8	−35.6
13	6	7	48.2	12.5	−12.6	−33.8	17	6	11	54.2	13.3	−12.7	−35.6
13	6	8	38.6	12.4	−7.3	−33.7	17	6	12	44.9	13.3	16.5	−35.6
13	7	6	36.2	12.6	−6.9	−34.0	17	7	10	42.6	13.3	−7.4	−35.6
13	7	7	33.8	12.5	−5.1	−33.9	17	7	11	23.8	13.3	6.8	−35.6
13	8	5	29.5	12.7	−3.1	−34.2	17	8	9	18.9	13.3	−5.4	−35.6
13	8	6	27.7	12.6	−3.8	−34.1	17	8	10	17.2	13.3	−0.9	−35.6
13	9	4	22.8	12.7	−3.5	−34.4	17	10	7	14.8	13.3	−1.8	−35.6
13	9	5	22.8	12.7	−3.5	−34.3	18	0	18	11.7	13.3	−1.3	−35.6
13	10	3	19.1	12.8	−3.4	−34.6	18	1	17	11.6	13.3	−1.3	−35.6
13	10	4	17.6	12.8	−3.2	−34.5	18	1	18	9.8	13.3	−1.7	−35.6
13	11	2	13.2	12.9	−1.4	−34.8	18	2	16	8.6	13.3	−2.1	−35.6
13	11	3	13.2	12.9	−1.4	−34.7	18	2	17	14.2	13.3	−2.6	−35.6
13	12	1	7.0	13.0	−2.8	−35.0	18	3	15	17.9	13.3	4.8	−35.6
13	12	2	7.0	12.9	−2.8	−34.9	18	3	16	16.4	13.3	−2.3	−35.6
13	13	0	3.2	13.1	0.3	−35.2	18	4	14	22.9	13.3	11.4	−35.6
13	13	1	2.8	13.0	−0.5	−35.1	18	4	15	16.2	13.3	−4.7	−35.6
14	0	14	25.1	13.1	−2.2	−35.3	18	5	14	28.5	13.3	3.8	−35.6

Table 9 (*continued*)

J''	K''_a	K''_c	$\tilde{\gamma}^0_{f\leftarrow i}$	$\tilde{A}_{f\leftarrow i}$	$\tilde{\delta}^0_{f\leftarrow i}$	$\tilde{B}_{f\leftarrow i}$	J''	K''_a	K''_c	$\tilde{\gamma}^0_i$	$\tilde{A}_i$	$\tilde{\delta}^0_i$	$\tilde{B}_i$
14	1	13	21.0	13.2	−1.8	−35.5	18	6	13	33.5	13.3	12.0	−35.6
14	2	12	24.4	13.3	1.4	−35.6	18	7	12	24.2	13.3	6.2	−35.6
14	2	13	27.0	13.3	−1.6	−35.6	18	8	11	16.9	13.3	0.7	−35.6
14	3	11	34.7	13.3	5.1	−35.6	19	0	19	6.2	13.3	−1.8	−35.6
14	3	12	29.9	13.3	−0.8	−35.6	19	1	18	5.9	13.3	−2.7	−35.6
14	4	10	53.6	13.3	6.8	−35.6	19	1	19	6.2	13.3	−1.8	−35.6
14	4	11	32.5	13.3	−0.9	−35.6	19	2	17	12.2	13.3	−0.9	−35.6
14	5	9	62.2	13.3	−6.0	−35.6	19	2	18	5.9	13.3	−2.7	−35.6
14	5	10	33.7	13.3	−3.1	−35.6	19	3	17	14.2	13.3	−0.1	−35.6
14	6	8	50.7	13.3	−13.0	−35.6							
14	6	9	35.7	13.3	−7.0	−35.6							
14	7	7	34.7	13.3		−35.6							

Note: The semi-empirical coefficients are given in $10^{-3}\,cm^{-1}\,atm^{-1}$. A blank means that the average semi-empirical coefficients have already been determined in Table 4.

Table 10
Semi-empirical coefficients obtained from averaging data of Table 4 for each J'' quantum number, or by using the extrapolation described in Section 4.2.2

J''	$\tilde{\gamma}^0_J$	$\tilde{A}_J$
0	100.5	2.8
1	100.5	3.6
2	95.5	4.8
3	90.7	5.1
4	84.9	5.7
5	79.3	6.4
6	73.5	7.3
7	67.1	8.4
8	61.3	10.6
9	56.0	9.3
10	50.1	10.1
11	44.6	9.7
12	39.6	11.6
13	35.8	12.0
14	31.4	13.0
15	28.8	13.3
16	24.1	13.3
17	20.8	13.3
18	15.5	13.3
19	7.5	13.3
20	7.5	13.3
21	7.5	13.3
22	7.5	13.3
23	7.5	13.3
24	7.5	13.3

water vapor in mixtures with air, 14,339 air-broadened half-widths and 8925 air pressure-induced line shifts. Data, for transitions for which multiple measurements were made, were taken and an averaged half-width or pressure-induced line shift was determined with a corresponding uncertainty (see Ref. [22] for details). The resulting file is called the intercomparison database. In Fig. 6, the half-widths, γ_{obs}, from the intercomparison database are compared with those determined by the empirical coefficients, γ_{calc}, from Section 4.1. The solid line is the 45° line, i.e. $\gamma_{obs} = \gamma_{calc}$. There are 2553 half-widths compared with an average percent difference of 1.0 and a standard deviation (SD) of about 6.5%. Comparing measurement with half-widths determined from the empirical coefficients of Section 4.2.1 gives an average percent difference of 1.4 and a standard deviation of ~8% for 459 transitions. Using the empirical coefficients of Section 4.2.2, 165 transitions can be compared giving an average difference of 5.4% and a SD of 8.9%. For the half-widths determined by the methods of Section 4.2.3, too few comparisons are made to report statistics.

Similar comparisons were made for the line shifts. Fig. 7 is a plot of δ_{obs} vs. δ_{calc} where the calculated line-shift coefficients are from the method of Section 4.1. The solid line in the figure signifies $\delta_{obs} = \delta_{calc}$. Here the difference between δ_{obs} and δ_{calc} was considered for the statistics. The average deviation between the intercomparison database and the approximate line shifts comparing 630 points is $0.0017\,cm^{-1}\,atm^{-1}$ and the standard deviation is $0.0019\,cm^{-1}atm^{-1}$. For the line shifts determined by the method of Section 4.2.1, there are 45 comparisons with the intercomparison database giving an average deviation of $0.0020\,cm^{-1}\,atm^{-1}$ and a standard deviation of $0.0019\,cm^{-1}\,atm^{-1}$. Fig. 8 is a plot of this comparison. The figure shows that the approximate δ_{calc} yields a shift that is more negative than the measured value. Too few comparisons are made for coefficients determined by the methods of Sections 4.2.2 and 4.2.3 to report statistics.

Another comparison was recently performed using the new empirical calculation of Toth [23]. Note that the experimental results of Ref. [23] have been used in our semi-empirical calculation.

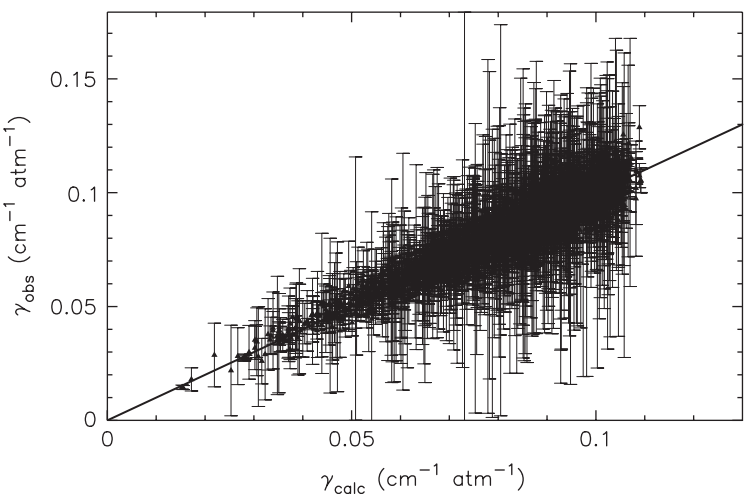

Fig. 6. Measured intercomparison database air-broadened half-widths, γ_{obs}, vs. γ_{calc} determined by the empirical coefficients, from Section 4.1. The solid line in the figure signifies $\gamma_{obs} = \gamma_{calc}$.

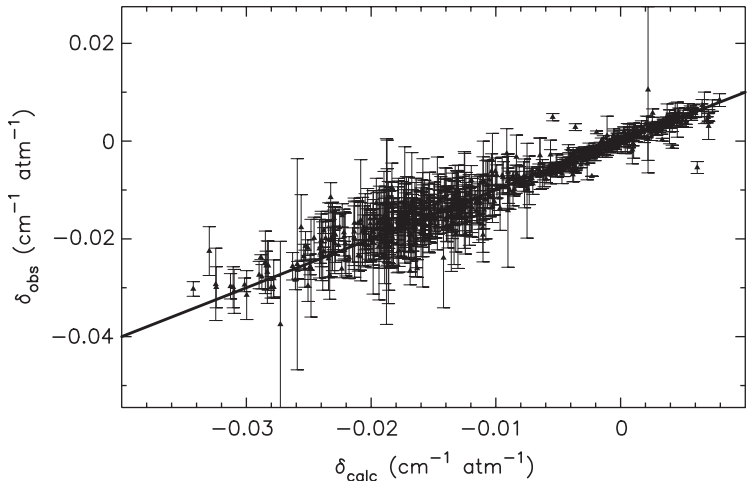

Fig. 7. Measured intercomparison database air pressure-induced line shifts, δ_{obs}, vs. δ_{calc} determined by the empirical coefficients from Section 4.1. The solid line in the figure signifies $\delta_{obs} = \delta_{calc}$.

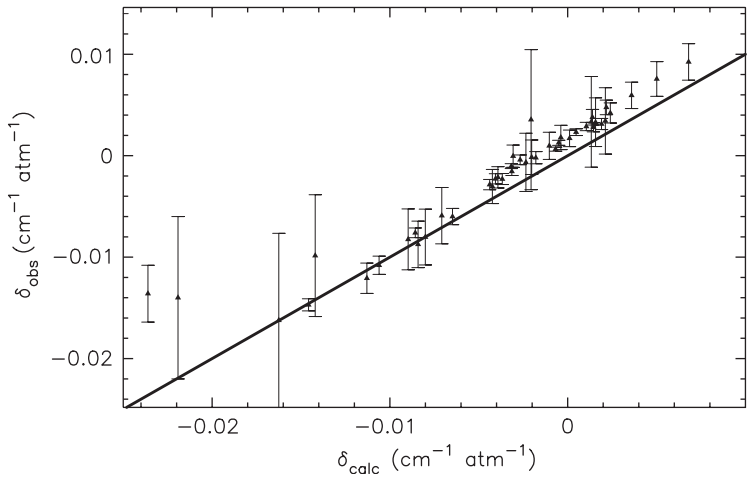

Fig. 8. Measured intercomparison database air pressure-induced line shifts, δ_{obs}, vs. δ_{calc} determined using the second level of approximation (Section 4.2.1). The solid line in the figure signifies $\delta_{obs} = \delta_{calc}$.

A complete comparison of the discrepancies both between the calculation and the measurements of Ref. [23], and between the calculation from this paper and those measurements, is presented in Figs. 9 and 10. Measurements for both γ_{air} and δ_{air} from Toth [23] are available for 4500 transitions between the 500 and 8000 cm^{-1} spectral region. Complete statistics show that the difference between Toth's calculation and Toth's measurements, and between this work and Toth's measurements, have the same order of magnitude. This is interesting especially if we consider that the semi-empirical functions used in this paper are only a function of vibrational quantum numbers, whereas the functions used by Toth [23] are only a function of rotational

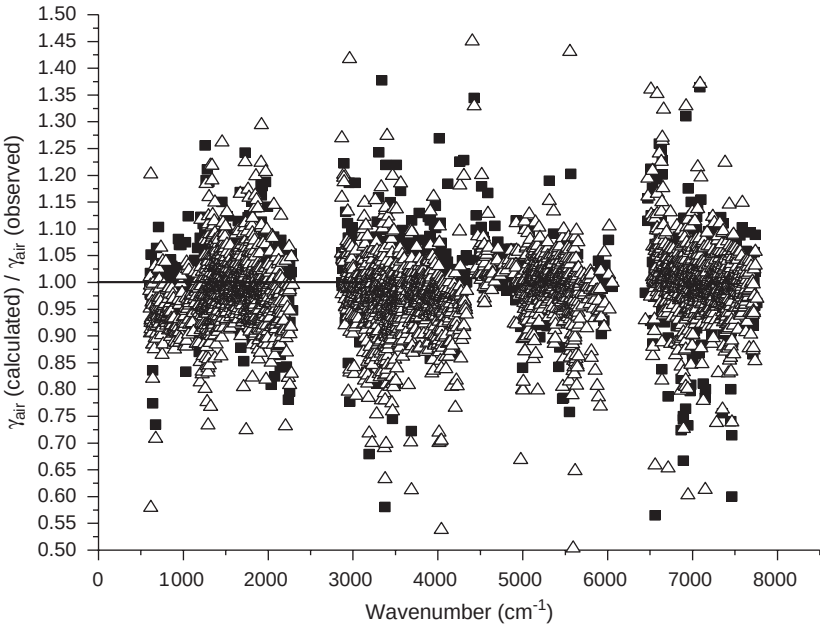

Fig. 9. Ratio for the air-broadened coefficients both between the calculation and the measurements of Toth [23] (solid squares), and between the calculations presented in this paper and the measurements [23] (open triangles).

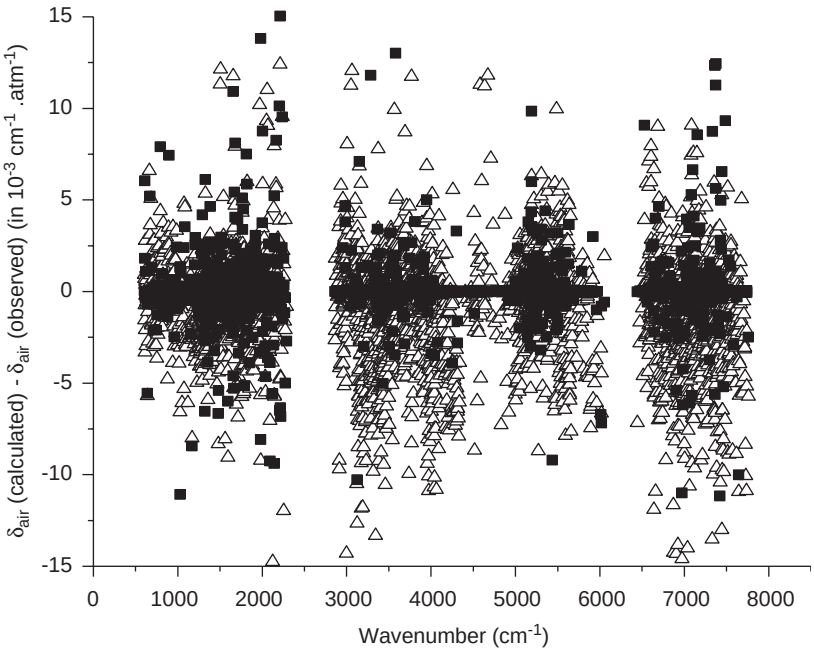

Fig. 10. Difference of the air pressure-induced shifts both between the calculation and the measurements of Toth [23] (solid squares), and between the calculations presented in this paper and the measurements [23] (open triangles).

quantum numbers. These comparisons only demonstrate that for an accuracy of ±5% for the air-broadened half-widths, the two models give similar results.

6. Conclusion

It should be emphasized that the work presented here is a first step in determining the half-widths and pressure-induced line shifts for the principal isotopologue of water vapor, $H_2^{16}O$. As new and better measurement and calculations become available, the parameters from this work will be updated using these improved data. A fit of air-broadened half-widths and air pressure-induced frequency shifts from experimental and theoretical works led to semi-empirical coefficients for about 700 sets of rotational quantum numbers. These semi-empirical coefficients allowed the calculation of γ_{air} and δ_{air} for any rovibrational transition corresponding to these sets of rotational quantum numbers, which corresponds to approximately half of the $H_2^{16}O$ transitions present in *HITRAN*.

Moreover, from averages of these semi-empirical coefficients, from measurements and calculations, and using approximations, we have determined approximate semi-empirical coefficients for the sets of rotational quantum numbers that were needed to have a complete set. This complete set of semi-empirical coefficients made it possible in principle to generate γ_{air} and δ_{air} for almost all transitions of $H_2^{16}O$ in *HITRAN*. A procedure was developed that added the air-broadened half-width and air pressure-induced line shift from a number of sources including: data from intercomparison of measurement (3541 transitions for γ_{air} and 680 transitions for δ_{air}) [22], data from the measurement database (14,355 transitions for γ_{air} and 8754 transitions for δ_{air}) [22], Toth's *smoothened* values (7716 transitions for γ_{air} and 2978 transitions for δ_{air}) [23], CRB calculations (6040 transitions for γ_{air} and 6040 transitions for δ_{air}) [12,13,18,24], and finally γ_{air} and δ_{air} presented in this work. Even with this new algorithm for half-widths and pressure-induced line shifts, the work developed here is used for 46.5% of the half-widths and 52.3% of the line shifts of $H_2^{16}O$ in *HITRAN* [1]. Note that 10.5% of the transitions still do not have line-shift data.

Semi-empirical half-widths and pressure-induced line shifts were determined for as many $H_2^{16}O$ transitions possible and, when no data were available from the algorithm discussed above, the semi-empirical values are used. It is interesting to note the proportion of line parameters determined in each of the steps. Of the 36,114 $H_2^{16}O$ transitions in the current *HITRAN* edition [1], 16,600 air-broadened half-widths and 19,387 air pressure-induced frequency shifts could be calculated using the semi-empirical coefficients obtained in step 1 (Section 4.1), 8662 air-broadened half-widths and 7895 air pressure-induced frequency shifts were calculated using the semi-empirical coefficients obtained in step 2 (Section 4.2.1), 5414 air-broadened half-widths and 3394 air pressure-induced frequency shifts were calculated using the semi-empirical coefficients obtained in step 3 (Section 4.2.2), 108 air-broadened half-widths and air pressure-induced frequency shifts were calculated using the semi-empirical coefficients obtained in step 4 (Section 4.2.3 with average values of the semi-empirical coefficients from Table 4), 1538 air-broadened half-widths and air pressure-induced frequency shifts have been calculated using the semi-empirical coefficients obtained in step 5 (Section 4.2.3 with average values of the semi-empirical coefficients from Table 9), and only 43 air-broadened half-widths have been calculated using the

semi-empirical coefficients obtained in step 6 (Section 4.2.3 with average values of the semi-empirical coefficients from Table 10) the case of high rotational quantum numbers. Note also that 3749 transitions of the $H_2^{16}O$ isotopologue are not assigned in *HITRAN* [1], and have a default value of $0.07\,cm^{-1}atm^{-1}$ for the air-broadened half-width.

In order to keep this update maintainable, a different reference has been used for the parameters determined from a different step of the calculation. With respect to the uncertainty, we used the same codes as those of *HITRAN*: we chose for the air-broadened half-widths a code 5 (accuracy between 5% and 10%) when this parameter has been obtained in step 1, a code 4 (between 10% and 20%) when it has been obtained in step 2, a code 4 (between 10% and 20%) when it has been obtained in step 3, and a code 3 (greater than 20%) when it has been obtained from steps 4 and 5 and code 2 (average or estimate) when it has been obtained from step 6. For the air pressure-induced frequency shifts, we chose a code 3 (accuracy between 0.001 and $0.01\,cm^{-1}atm^{-1}$) when this parameter has been obtained in step 1 or 2, and a code 2 (between 0.01 and $0.1\,cm^{-1}atm^{-1}$) when it has been obtained in steps 3, 4, or 5.

The new set of air-broadening half-widths and air-pressure shift frequency described in this paper has been tested using the Far Infrared high Resolution atmospheric Spectra recorded from the FIRS-2 balloon-borne interferometer [25]. FIRS-2 operates over the far-infrared wavelength region from 80 to $1400\,cm^{-1}$. The long wavelength part of the band is dominated by the rotational transitions of H_2O. Ref. [26] shows that introducing the calculation of the line-shape parameters determined in this work gave better results compared with the use of the coefficients from the previous *HITRAN* database [3], especially for limb-viewing spectra with tangent altitudes in the upper troposphere. It seems clear that the line-shape parameters determined in this work are an improvement over the values that were used on the previous versions of *HITRAN*. The use of these new parameters to supplement those from databases of measurement and CRB calculations should lead to a much improved set of line-shape parameters for water vapor.

These new air-broadened half-widths and air pressure-induced frequency shifts will contribute to improved atmospheric remote sensing, and will aid important experiments, for example the Earth Observing System (EOS) experiments [27], the National Polar-orbiting Operational Environmental Satellite System (NPOESS) [28], and the Michelson Interferometer for Passive Atmospheric Sounding (MIPAS) [29]. An identical study on the vibrational dependence of self-broadened half-widths is planned, and will lead to an update of these coefficients in a future *HITRAN* edition. The Tables presented in this paper are available in their complete form on request to the authors.

Acknowledgements

The authors thank L.R. Brown, M. Carleer, P.F. Coheur, M.-F. Mérienne, R.A. Toth, P. Varanasi, and Q. Zou for providing their results, sometimes prior to publication. The current effort has been supported by the NASA Earth Observing System (EOS), under the grant NAG5-13534, and funding from the Office of the Secretary of Defense (OSD) High Energy Laser Joint Technology Office. One of the authors (RRG) is pleased to acknowledge support of this research by the National Aeronautics and Space Administration (NASA) through Grant No. NAG5-11064 and by the National Science Foundation (NSF) through Grant No. ATM-0242537.

References

[1] Rothman LS, Jacquemart D, Barbe A, Benner DC, Birk M, Brown LR, Carleer MR, Chackerian C, Chance K, Coudert LH, Dana V, Devi VM, Flaud JM, Gamache RR, Goldman A, Hartmann JM, Jucks KW, Maki AG, Mandin JY, Massie ST, Orphal J, Perrin A, Rinsland CP, Smith MAH, Tennyson J, Tolchenov RN, Toth RA, Vander Auwera J, Varanasi P, Wagner G. The HITRAN 2004 molecular spectroscopic database. JQSRT, this issue.

[2] Bernath PF. The spectroscopy of water vapour: experiment, theory and applications. Phys Chem Chem Phys 2002;4:1501–9.

[3] Rothman LS, Barbe A, Benner DC, Brown LR, Camy-Peyret C, Carleer MR, Chance KV, Clerbaux C, Dana V, Devi VM, Fayt A, Flaud JM, Gamache RR, Goldman A, Jacquemart D, Jucks KW, Lafferty WJ, Mandin JY, Massie ST, Nemtchinov V, Newnham D, Perrin A, Rinsland CP, Schroeder J, Smith K, Smith MAH, Tang K, Toth RA, Vander Auwera J, Varanasi P, Yoshino K. The HITRAN molecular spectroscopic database: edition of 2000 including updates through 2001. JQSRT 2003;82:5–44.

[4] Grossmann BE, Browell EV. Water vapor line broadening and shifting by air, nitrogen, oxygen, and argon in the 720-nm wavelength region. J Mol Spectrosc 1989;138:562–95.

[5] Remedios JJ. DPhil Thesis. Oxford University; 1990.

[6] Toth RA. Air- and N_2-broadening parameters of water vapor: 604 to 2271 cm^{-1}. J Mol Spectrosc 2000;201:218–43.

[7] Brown LR, Toth RA, Dulick M. Empirical line parameters of $H_2^{16}O$ near 0.94 μm: positions, intensities and air-broadening coefficients. J Mol Spectrosc 2002;212:57–82.

[8] Gamache RR, Davies RW. Theoretical calculations of N_2-broadened halfwidths of H_2O using quantum Fourier transform theory. Appl Opt 1983;22:4013–9.

[9] Gamache RR. Unpublished data.

[10] Robert D, Bonamy J. Short range force effects in semiclassical molecular line broadening calculations. J Phys 1979;40:923–43.

[11] Gamache RR, Lynch R, Neshyba SP. New developments in the theory of pressure-broadening and pressure-shifting of spectral lines of H_2O: the complex Robert–Bonamy formalism. JQSRT 1998;59:319–35.

[12] Gamache RR, Hartmann JM. Collisional parameters of H_2O lines: effects of vibration. JQSRT 2004;83:119–47.

[13] Gamache RR, Fischer J. Half-widths of $H_2^{16}O$, $H_2^{18}O$, $H_2^{17}O$, $HD^{16}O$, and $D_2^{16}O$: I. Comparison between isotopomers. JQSRT 2003;78:289–304.

[14] Toth RA. Private communication (2004).

[15] Fally S, Coheur PF, Carleer M, Clerbaux C, Colin R, Jenouvrier A, Mérienne MF, Hermans C, Vandaele AC. Water vapor line broadening and shifting by air in the 26000–13000 cm^{-1} region. JQSRT 2003;82:119–31.

[16] Mérienne MF, Jenouvrier A, Hermans C, Vandaele AC, Carleer M, Clerbaux C, Coheur PF, Colin R, Fally S, Bach M. Water vapor line parameters in the 13 000–9250 cm^{-1} region. JQSRT 2003;82:99–117.

[17] Zou Q, Varanasi V. Laboratory measurement of the spectroscopy line parameters of water vapor in the 610–2100 and 3000–4050 cm^{-1} regions at lower-tropospheric temperatures. JQSRT 2003;82:45–98.

[18] Gamache RR, Fischer J. Calculated half-widths and line shifts of water vapor transitions in the 0.7 μm region and a comparison with published data. J Mol Spectrosc 2001;207:254–62.

[19] Gamache RR, Lynch R, Plateaux JJ, Barbe A. Halfwidths and line shifts of water vapor broadened by CO_2: measurements and complex Robert–Bonamy formalism calculations. JQSRT 1997;57:485–96.

[20] Devi VM, Benner DC, Smith MAH, Rinsland CP. Measurements of pressure broadening and pressure shifting by nitrogen in the v_1 and v_3 bands of $H_2^{16}O$. J Mol Spectrosc 1992;155:333–42.

[21] Tolchenov RN, Zobov NF, Polyansky OL, Tennyson J, Naumenko O, Carleer M, Coheur PF, Fally S, Clerbaux C, Jenouvrier A, Vandaele AC. Water vapor line assignments in the 9250–26000 cm^{-1} frequency range. J Mol Spectrosc, 2005, in press.

[22] Gamache RR, Hartmann JM. An intercomparison of measured pressure-broadening and pressure-shifting parameters of water vapor. Can J Chem 2004;82:1013–27.

[23] Toth RA. Measurements and analysis (using empirical functions for widths) of air- and self-broadening parameters of H_2O. JQSRT, 2005;94:1–50.

[24] Gamache RR. Line shape parameters for water vapor in the 3.2 to 17.76 μm region for atmospheric applications. J Mol Spectrosc 2005;229:9–18.
[25] Johnson DG, Jucks KW, Traub WA, Chance KV. Smithsonian stratospheric far-infrared spectrometer and data reduction system. J Geophys Res 1995;100:3091–106.
[26] Jucks K. Comparison of far infrared high-resolution spectra with new parametrizations for H_2O and other molecules. Poster PW2, The eighth HITRAN database conference, Cambridge MA, USA, 16–18 June 2004.
[27] King MD, Herring DD, Diner DJ. The Earth Observing System: a space-based program for assessing mankind's impact on the global environment. Opt Photon News 1995;6:34–9.
[28] Jones D. NPOESS the next generation earth observation system. Earth Observat Mag 2004;13:4–10.
[29] Flaud JM, Piccolo C, Carli B, Perrin A, Coudert LH, Teffo JL, Brown LR. Molecular line parameters for the MIPAS (Michelson Interferometer for Passive Atmospheric Sounding) experiment. Atmos Oceanic Opt 2003;16:172–81.